

Article

Evaluation and Comparison of Six High-Resolution Daily Precipitation Products in Mainland China

Xiaoran Wu ^{1,2}  and Na Zhao ^{1,2,3,*} ¹ State Key Laboratory of Resources and Environmental Information System, Institute of Geographic Sciences and Natural Resources Research, Chinese Academy of Sciences, Beijing 100101, China² College of Resources and Environment, University of Chinese Academy of Sciences, Beijing 100049, China³ Jiangsu Center for Collaborative Innovation in Geographic Information Resource Development and Application, Nanjing 210023, China

* Correspondence: zhaon@lreis.ac.cn

Abstract: Satellite-based and reanalysis precipitation products have experienced increasing popularity in agricultural, hydrological and meteorological applications, but their accuracy is still uncertain in different areas. In this study, six frequently used high-resolution daily precipitation products, including Climate Hazards Group InfraRed Precipitation with Station data (CHIRPS), Global Satellite Mapping of Precipitation (GSMaP), Integrated Multi-satellitE Retrievals for Global Precipitation Measurement (IMERG), Multi-Source Weighted-Ensemble Precipitation (MSWEP), Precipitation Estimation from Remotely Sensed Information using Artificial Neural Networks-Cloud Classification System-Climate Data Record (PERSIANN-CCS-CDR) and European Center for Medium-Range Weather Forecasts Reanalysis V5-Land (ERA5-Land), were comprehensively evaluated and compared in nine regions of mainland China between 2015 and 2019. The results reveal that, in general, GSMAp is the best precipitation product in different agricultural regions, especially based on the Pearson correlation coefficient (CC) and critical success index (CSI). ERA5-Land and MSWEP tend to have the highest probability of detection (POD) values, and MSWEP tends to have the smallest relative root mean squared error (RRMSE) values. GSMAp performs better at almost all precipitation levels and in most agricultural regions in each season, while MSWEP has the best performance for capturing the time series of mean daily precipitation. In addition, all precipitation products perform better in summer and worse in winter, and they are more accurate in the eastern region. The findings of this study will contribute to understanding the uncertainties of precipitation products, improving product quality and guiding product selection.



Citation: Wu, X.; Zhao, N. Evaluation and Comparison of Six High-Resolution Daily Precipitation Products in Mainland China. *Remote Sens.* **2023**, *15*, 223. <https://doi.org/10.3390/rs15010223>

Academic Editors: Kenji Nakamura and Yuanjian Yang

Received: 21 November 2022

Revised: 28 December 2022

Accepted: 28 December 2022

Published: 31 December 2022



Copyright: © 2022 by the authors. Licensee MDPI, Basel, Switzerland. This article is an open access article distributed under the terms and conditions of the Creative Commons Attribution (CC BY) license (<https://creativecommons.org/licenses/by/4.0/>).

1. Introduction

Precipitation is a crucial meteorological variable that plays a vital role in the hydrological cycle, agriculture and eco-environment systems [1–3]. The spatiotemporal distribution of precipitation has profound impacts on meteorology and hydrology and their associated processes [4,5]. Therefore, precise estimation of precipitation including the intensity and frequency is of great importance. However, due to the strong spatial and temporal variability of precipitation, high-quality estimation of precipitation at fine spatial and temporal resolutions remains a great challenge [6,7].

Conventional rain gauges have the most accurate observations at station locations [8], but it is difficult to obtain high-resolution daily precipitation distribution data over large areas due to the strong spatial and temporal variability of daily precipitation [9,10] and the low-density rain gauge network [11,12]. In addition, rain gauges often suffer from frequent time-series gaps [11,12], and many of them only have short historical records [13].

In recent decades, many satellite-based and reanalysis high-resolution precipitation products have been released [14], including Climate Hazards Group InfraRed Precipitation

with Station data (CHIRPS) [15], Global Satellite Mapping of Precipitation (GSMP) [16], Integrated Multi-satellitE Retrievals for Global Precipitation Measurement (IMERG) [17], Multi-Source Weighted-Ensemble Precipitation (MSWEP) [18], Precipitation Estimation from Remotely Sensed Information using Artificial Neural Networks-Cloud Classification System-Climate Data Record (PERSIANN-CCS-CDR) [19] and European Center for Medium-Range Weather Forecasts Reanalysis V5-Land (ERA5-Land) [20]. Some of them have been widely applied in agriculture [21,22], climate [23,24] and hydrology [25,26]. Nevertheless, numerous studies have shown that the performance of precipitation products produced based on different sensors and retrieval algorithms varies considerably and that there is no optimal product in all cases [27–32]. Therefore, there remains a need to evaluate and compare the precipitation products with fine spatial and temporal resolutions in different regions, times and precipitation levels [6,7,33,34].

Many studies have been conducted to examine the error characteristics of precipitation products at different temporal and spatial scales. In the Adige Basin, CHIRPS was shown to be the best product, and all products tended to show larger errors in the winter months in terms of overall statistical metrics [34]. A study conducted in Australia concluded that IMERG better characterized the distribution of precipitation compared to Tropical Rainfall Measurement Mission (TRMM), Multi-satellite Precipitation Analysis (TMPA), Climate Prediction Center morphing method (CMORPH), PERSIANN and PERSIANN-CDR [29]. Another evaluation carried out in the USA found that GSMP was more accurate than others, and all the compared datasets exhibited underestimation in winter yet overestimation in summer [35]. In addition, several precipitation products released in recent years have been shown to perform better than previous products in some regions. For example, the accuracy of CHIRPS and MSWEP was compared on the Tibetan Plateau, and the results showed that MSWEP was more accurate [36]. ERA5-Land has a higher spatial resolution and better precipitation estimates than ERA5 in most regions [20]. PERSIANN-CCS-CDR was found to perform better than PERSIANN-CDR in the USA in terms of the resolution, intensity and spatial patterns of precipitation [19]. These studies have not only demonstrated the considerable temporal and spatial variation in the performance of precipitation products but have also identified relatively accurate high-resolution precipitation products as well as those released in recent years with excellent preliminary evaluation but not yet fully assessed.

Located in the eastern part of Eurasia and west of the Pacific Ocean, China is one of the countries with the most significant monsoons in the world. Many factors, such as the vast area, complex topography and strong monsoon, contribute to the significant spatial variation in precipitation of China [37,38], which decreases unevenly from the southeastern coast to the northwestern interior [39]. In addition, both the amount and spatial variability of precipitation differ significantly among seasons [40]. Therefore, a temporal and spatial evaluation of precipitation products helps to provide a relatively optimal precipitation product for regional studies. A few studies evaluating precipitation products in mainland China have been reported in the literature. A drought monitoring study compared the reliability level of seventeen monthly precipitation products in drought detection [32]. A quantitative analysis of the GPM-based precipitation products pointed out that the overall quality of GSMP was slightly superior to IMERG in eastern and southern China [41]. IMERG was found to be more accurate than TMPA in the major basins of mainland China [31]. However, many studies are limited to two or three precipitation products, ignoring other available prominent high-quality datasets. In addition, few attempts have been made to evaluate the estimates of daily precipitation over China, despite its important role in agriculture and vegetation phenology [42,43]. Furthermore, most of the previous studies paid attention to a local area of China, while no studies attempted to identify the error characteristics of precipitation products in different agricultural regions, although many agricultural studies were carried out in a specific agricultural region [44–47]. To date, to the best of our knowledge, this is the first time that the promising high-resolution daily precipitation products have been evaluated and compared in different agricultural

regions in mainland China, which provides important data support in different agricultural regions for agricultural research such as crop yield estimation, sustainable agricultural development and crop adaptation to climate change [21,22].

Here, we present the evaluation and comparison of six high-quality daily precipitation products in nine regions of mainland China. Five satellite-based precipitation products (CHIRPS, GSMP, IMERG, MSWEP and PERSIANN-CCS-CDR) and a reanalysis precipitation product (ERA5-Land) with the spatial resolution equal to or finer than 0.1° were selected based on their good performance demonstrated by previous studies [18–20,28,29,34]. The spatial and temporal performance of these prominent precipitation products were evaluated and compared against 2413 rain gauge stations at a daily scale between 2015 and 2019. The rest of this paper is organized as follows. Section 2 describes the study area, precipitation products and evaluation metrics. Section 3 focuses on the assessment results. The discussion and conclusion are given in Sections 4 and 5, respectively.

2. Materials and Methods

2.1. Study Area

China has a land area of approximately 9.6 million km², most of which is located in the midlatitudes. As depicted in Figure 1, the terrain of mainland China, ranging from -268 to 8405 m, is very complex and can be abstracted into three great steps from west to east. Many factors, such as complex topography, volatile monsoon (both its intensity and direction) and geographic location, contribute to the significant spatial variation in China's climate, with mean annual temperature and precipitation decreasing in general from the south to north and from the southeastern coast to the northwestern interior, respectively [38,39,48]. To better reveal the performance of precipitation products in different regions, we adopted a zoning system that divides mainland China into nine agricultural regions with similar temperature, precipitation and soil regimes [49,50]. The nine regions are the Inner Mongolia Plateau, the Gan-Xin Desert Plateau, the Northeast Plain, the Loess Plateau, the Qinghai-Tibet Plateau, the Sichuan Basin and the Yunnan-Guizhou Plateau, the South China Tropical Crops Region, the Huang-Huaihai Plain and the Middle and Lower Yangtze River Region. They were termed R_i, $i = 1, 2 \dots, 9$, respectively, in this study (Figure 1). We further group these regions into the northeastern region (R₁ and R₃), western region (R₂ and R₅), central region (R₄ and R₆) and eastern region (R₇, R₈ and R₉) to better represent spatial patterns. In particular, the southern region includes R₆, R₇ and R₉, and the northern region includes R₁, R₂ and R₈.

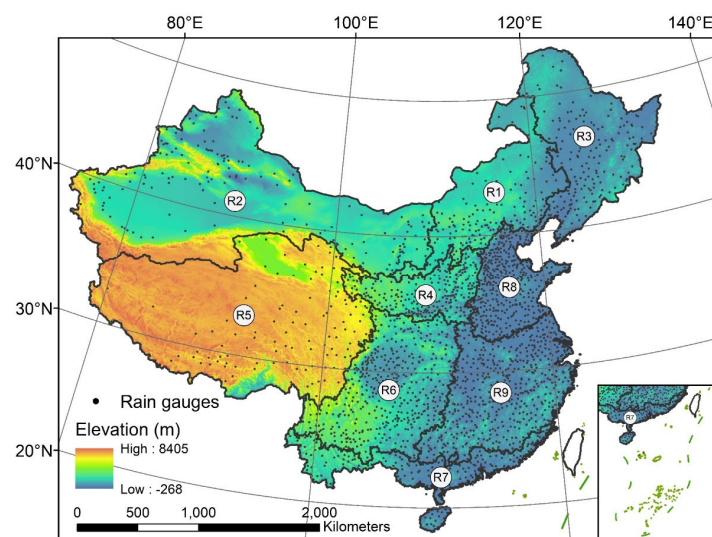


Figure 1. Digital elevation model and the location of the nine agricultural regions of mainland China, together with the distribution of 2413 rain gauges throughout mainland China.

2.2. Datasets

2.2.1. Rain Gauge Measurements

The daily precipitation data from the high-density rain gauge dataset, obtained from the National Meteorological Information Center of the China Meteorological Administration (CMA), was revised and checked under strict quality control before being released. Currently, it is deemed the best ground truth of daily precipitation [37,51]. We removed the stations with time coverage less than 95% during the study period to ensure continuity of observation series. Finally, a total of 2413 stations throughout mainland China were used as the reference data to evaluate the precipitation products, whose locations are shown in Figure 1.

2.2.2. CHIRPS

CHIRPS is a 35+ year quasi-global rainfall dataset spanning 50°S–50°N from 1981 to near-present, which integrates in-house climatology, CHPclim, satellite imagery, and rain gauge data [15]. The latest version, CHIRPS V2.0, was released in February 2015 and seems well suited to monitoring droughts in regions where Cold Cloud Duration (CCD) estimates relate reasonably well to observed precipitation systems [15]. The finest spatial resolution of CHIRPS is 0.05°.

2.2.3. GSMAp

Sponsored by the Japan Science Technology Agency (JST) and the Japan Aerospace Exploration Agency (JAXA) [52], GSMAp aims to develop a precise high-resolution global precipitation product by integrating various PMW/IR sensors [16]. GSMAp V7 includes the near-real-time product (GSMAp_NRT), microwave-IR combined product (GSMAp_MVK) and gauge-calibrated rainfall product (GSMAp_Gauge). In this study, GSMAp_Gauge, adjusted by Climate Prediction Center (CPC) global daily gauge data [53,54], was evaluated.

2.2.4. IMERG

IMERG is the level-3 algorithm of Global Precipitation Measurement (GPM), which combines all microwave estimates of the GPM constellation, infrared estimates and precipitation gauge analyses [55]. Three products (IMERG-E, IMERG-L and IMERG-F) are given in the latest IMERG version (V06B) [17]. They are processed by different algorithms, and the last one has the best performance most of the time [56,57]. Therefore, IMERG-F was assessed and compared in this study across China, with a spatial resolution of 0.1°.

2.2.5. MSWEP

To optimally combine data from various gauge, satellite, and reanalysis data sources, including CMORPH, daily gauge data, ERA-Interim, GSMAp, etc., MSWEP was generated through four stages of merging [58]: (i) producing a global map of long-term mean precipitation; (ii) merging precipitation anomalies from the different datasets for each data source; (iii) merging the precipitation anomalies from the different data sources; and (iv) downscaling the long-term mean precipitation to a finer timescale. The latest version, MSWEP V2, is the first fully global precipitation dataset with a 0.1° spatial resolution [18].

2.2.6. PERSIANN-CCS-CDR

Most available high-resolution data are of short-term duration, yet the long-term duration data are of low resolution [59]. PERSIANN-CCS-CDR was designed to address these limitations [19] and was released in 2021. The finest spatial resolution of PERSIANN-CCS-CDR is 0.04°, and it has a long-term time series from 1983 to the present, spanning 60°S–60°N. An evaluation showed that PERSIANN-CCS-CDR performed better than PERSIANN-CDR in most cases, especially for extreme events [19]. However, to date, very few evaluations have compared this dataset with other excellent precipitation products, despite its great potential performance. We assessed PERSIANN-CCS-CDR across China in detail for the first time.

2.2.7. ERA5-Land

ERA5, the fifth generation of ECMWF, provides a large number of atmospheric, land and oceanic climate variables, with much higher spatial and temporal resolutions than ERA-Interim [60]. ERA5-Land is a reanalysis dataset reproduced from ERA5 at a 0.1° spatial resolution [20]. Different from satellite precipitation products, reanalysis precipitation products incorporate multiple surface variables using the laws of physics. ERA5-Land was chosen in this study due to its excellent performance reported in other studies [61,62].

2.3. Methodology

2.3.1. Preprocessing

Some previous studies upscaled the rain gauges to the same grid scale as the precipitation products through various interpolation methods to address the scale mismatch issue [63,64]. However, the uncertainty of the results has not been well assessed at present due to the uncertainties introduced by interpolation [65,66]. Instead, followed by other researchers [31,56,65–68], we adopted a widely-used simple approach where the average of the rain gauge measurements within each pixel was used as a reference for this pixel. In addition, the spatial resolution of the precipitation products chosen in this study ranges from 0.04° to 0.1° . We did not upscale or downscale the products into the same resolution, because of the uncertainty arising from the scale transformation process [65]. Followed by the method used in some previous studies [23,56,65], the high-density validation stations were processed against the pixel size of each precipitation product separately in this study, and finally, the error values calculated from the precipitation products were compared.

2.3.2. Evaluation Metrics

To evaluate the accuracy and precipitation detection capability of the precipitation products, four metrics, including the Pearson correlation coefficient (CC), relative root mean squared error (RRMSE), probability of detection (POD) and critical success index (CSI), were used in this study. CC, ranging from -1 to 1 , quantifies the degree of linear correlation between precipitation products and rain gauge observations. RRMSE is used to measure error, reflecting the degree of deviation. POD indicates the proportion of hits in precipitation events, and a high POD value is expected. The CSI takes into account hits, misses and false alarms and is sensitive to the climatological frequency of events. To quantify the detection capability of precipitation events, we adopted 0.1 mm/d as the precipitation threshold according to the CMA (<http://zwgk.cma.gov.cn/>, accessed on 12 April 2022). The formulas of the evaluation metrics are listed in Table 1.

Table 1. Evaluation metrics used in this study. P and G mean products and rain gauge observation, respectively. Hits, Misses and False alarms in the table refer to the observed precipitation correctly detected by products, observed precipitation missed by products and the precipitation detected by the products but not observed by the rain gauge, respectively.

Metric	Formula	Optimal
Pearson correlation coefficient (CC)	$CC = \frac{\sum_{i=1}^n (G_i - \bar{G})(S_i - \bar{S})}{\sqrt{\sum_{i=1}^n (G_i - \bar{G})^2} \cdot \sqrt{\sum_{i=1}^n (S_i - \bar{S})^2}}$	1
relative root mean squared error (RRMSE)	$RRMSE = \sqrt{\frac{\sum_{i=1}^n (P_i - G_i)^2}{n}} / \frac{\sum_{i=1}^n G_i}{n}$	0
probability of detection (POD)	$POD = \frac{Hits}{Hits+Misses}$	1
critical success index (CSI)	$CSI = \frac{Hits}{Hits+False\;alarms+Misses}$	1

3. Results

3.1. Overall Performance of Precipitation Products throughout Mainland China

3.1.1. Average Accuracy of Precipitation Products

To quantify the average accuracy of these products, the error and precipitation detection capability of the six products are listed in Table 2, which shows that GSMAp yields the highest CC and CSI with values of 0.55 and 0.48, respectively. The RRMSE values of MSWEP (3.09) and GSMAp (3.10) are much smaller than the others. ERA5-Land has the highest POD (0.79), followed by MSWEP (0.78) and GSMAp (0.76). According to these four metrics, CHIRPS and PERSIANN-CCS-CDR perform much worse than the others in terms of average accuracy, with lower CC, POD and CSI and higher RRMSE. In contrast, GSMAp is the best product in general, with a higher average accuracy. Additionally, MSWEP and ERA5-Land also perform well.

Table 2. Mean values of CC, RRMSE, POD and CSI of six products based on all observations between 2015 and 2019. We collected all corresponding samples and calculated the statistics at once to avoid unstable statistics caused by too few precipitation samples on some days.

Product	CC	RRMSE	POD	CSI
CHIRPS	0.34	4.23	0.35	0.25
ERA5-Land	0.50	3.20	0.79	0.45
GSMAp	0.55	3.10	0.76	0.48
IMERG	0.47	3.58	0.62	0.39
MSWEP	0.52	3.09	0.78	0.46
PERSIANN-CCS-CDR	0.27	4.16	0.43	0.27

3.1.2. Performance of Precipitation Products for Different Precipitation Levels

In this study, we divide the rate of daily precipitation into five levels (<0.1 mm/d, 0.1–10 mm/d, 10–25 mm/d, 25–50 mm/d and >50 mm/d) according to the CMA and the number of observations. These five levels are named as no rain, light rain, moderate rain, heavy rain and violent rain, respectively.

Figure 2 presents the probability density functions (PDFs) of the daily precipitation rate of the rain gauges and the six precipitation products. As shown in the figure, the number of precipitation events (>0.1 mm/d) accounts for only 31.83% of all observations. Overall, all precipitation products capture the precipitation frequency characteristics of moderate, heavy and violent rain well, with a bias of less than 2% from the truth. The errors come mainly from the estimation of no rain and light rain. In this study, CHIRPS shows an overestimation of 12.68% of the no rain and an underestimation of 14.40% of the light rain. A very similar result was also reported in the Adige Basin [34]. In contrast, all products, except CHIRPS, underestimate the no rain and overestimate the light rain, with the most serious case occurring in ERA5-Land and MSWEP, which underestimate the no rain by 23.10% and 21.32% and overestimate the light rain by 20.98% and 21.21%, respectively. For PERSIANN-CDR, poor classification accuracy was found in both Malaysia [57] and the Adige Basin [34]. However, PERSIANN-CCS-CDR performs very well in all intervals throughout mainland China, with a mean bias of only 0.46%. This shows that PERSIANN-CCS-CDR, the latest product of the PERSIANN family, may achieve a significant improvement in classification accuracy.

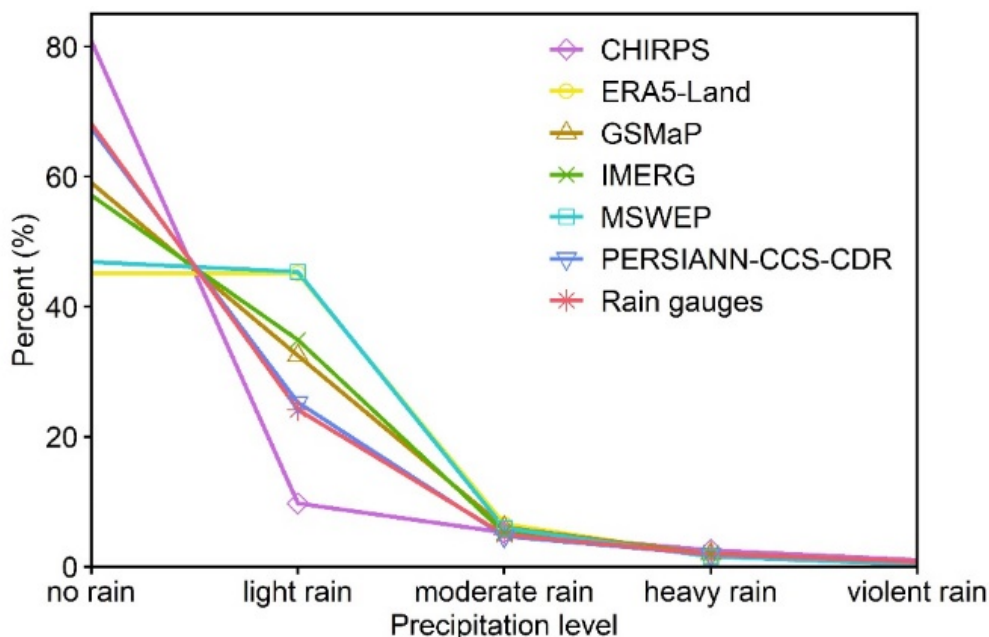


Figure 2. Probability density function of the daily precipitation rate of rain gauges and six precipitation products between 2015 and 2019.

The results of four statistical metrics of different precipitation levels are displayed in Figure 3. Compared to considering all precipitation levels, the correlation between products and rain gauges decreases significantly at individual precipitation levels. All products have the highest CC for violent rain and a relatively high CC for light rain, with mean CC values of 0.26 and 0.18. In terms of CC, GSMaP is the best product at all precipitation levels (CC values are 0.24, 0.15, 0.13 and 0.34, respectively), followed by MSWEP. CC values are very low in all groups compared to previously reported overall CC and seasonal CC. This is because CC is the consistency of the variability of the two variables: at overall CC or seasonal CC, the interval of variability of daily precipitation is larger and the effect of the uncertainty of the estimates is reduced. However, after dividing the daily precipitation into several precipitation levels, the interval of variation of precipitation in each level becomes smaller, which leads to uncertainty in the estimates affecting the CC values even more. The results of RRMSE show that all products have the largest RRMSE for light rain, led by CHIRPS (4.56) and followed by PERSIANN-CCS-CDR (4.07) and IMERG (3.69). This indicates that precipitation products still have large uncertainties in estimating light rain. Furthermore, MSWEP has the lowest RRMSE values of 2.72 and 0.78 for light rain and moderate rain, respectively, and GSMaP performs the best for heavy rain and violent rain, with RRMSE values of 0.69 and 0.75, respectively. A common feature is that these products are more capable of identifying light rain than other precipitation levels, and the performance decreases with increasing precipitation rate, which is consistent with studies in the central United States [69]. Based on POD, MSWEP and ERA5-Land identify a higher proportion of light rain than other products, with values of 0.73 and 0.71, respectively, while IMERG and GSMaP perform better at higher precipitation levels (heavy rain and violent rain). However, GSMaP has the highest CSI at all precipitation levels, with values of 0.37, 0.17, 0.13 and 0.15, respectively, which indicates that ERA5-Land and MSWEP have more false alarms for light rain. Overall, GSMaP is better than the others at all precipitation levels, while MSWEP has an advantage over GSMaP in terms of RRMSE and POD for light rain. The improved performance of GSMaP for light rain could mainly benefit from the fact that the GPM combined instrument (GMI) sensor is significantly better than the TRMM combined instrument (TMI) at capturing light precipitation [70].

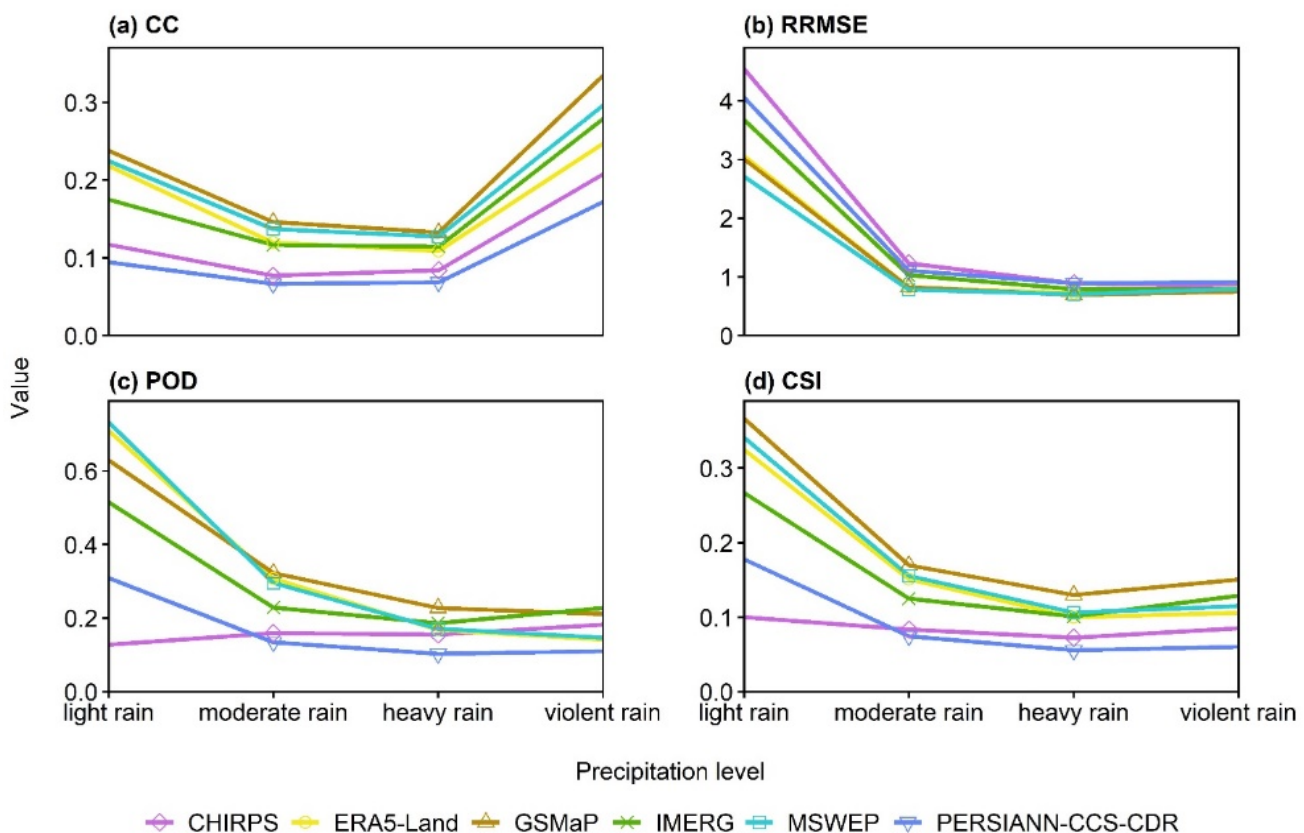


Figure 3. Mean values of four statistical metrics of precipitation products at four precipitation levels between 2015 and 2019. From left to right and top to bottom: (a) CC, (b) RRMSE, (c) POD and (d) CSI.

3.1.3. Performance of Precipitation Products in Different Seasons

Figure 4 presents the time series of the mean daily precipitation of rain gauges and six precipitation products. In general, the time series are unimodal, with precipitation peaking on the period of the 170th day to the 230th day (mean precipitation is 5.20 mm/d), and each product is consistent with the rain gauge observations. CHIRPS and PERSIANN-CCS-CDR, however, have significantly more outliers overestimating the precipitation than the other products around July. Specifically, they overestimate precipitation by more than 1 mm/d for 40.98% and 34.43% of the period of the 170th day to the 230th day, respectively. Overestimation by CHIRPS in the wet season was also reported in Colombia but not in Peru and Turkey [15,71], indicating that CHIRPS does not overestimate the precipitation in all areas during the wet season. In addition, CHIRPS yields one or several significant overestimates (2 mm/d higher than rain gauges) in almost every month. PERSIANN-CCS-CDR shows a mean underestimation of 0.32 mm/d and 0.50 mm/d in March and October, respectively. Overestimations of daily precipitation exist in GSMAp and IMERG throughout the year, similar to ERA5-Land, but more slightly, with mean overestimation values of 0.06 mm/d, 0.08 mm/d and 0.10 mm/d, respectively. In contrast, MSWEP is an excellent product to capture the characteristics of the time series, with a mean overestimation of only 0.01 mm/d and very few overestimations or underestimations exceeding 1 mm/d, which perhaps benefits from the fact that it incorporates data from multiple sources in a weighted manner [58].

The seasonal variations in accuracy and precipitation detection capability are presented in Table 3. Overall, the performance of the six precipitation products varies among seasons, but their performance ranking is stable, with GSMAp being the best and CHIRPS being the worst. In terms of CC, GSMAp, MSWEP, ERA5-Land and IMERG perform much better than CHIRPS and PERSIANN-CCS-CDR in all seasons, with GSMAp having the highest CC values of 0.53, 0.52, 0.58 and 0.68, respectively. The RRMSE values of MSWEP, GSMAp

and ERA5-Land are smaller than the other precipitation products in all seasons, with the smallest RRMSE values in spring, summer and autumn being MSWEP with 2.95, 2.51 and 3.01, respectively, and the smallest RRMSE in winter being GSMAp (3.55). ERA5-Land, MSWEP and GSMAp have significant advantages in terms of POD compared to other precipitation products. ERA5-Land has the highest POD in summer, autumn and winter with 0.84, 0.78 and 0.71, respectively, while MSWEP performs best in spring with a POD of 0.77. Based on CSI, GSMAp outperforms other products in all seasons, with values of 0.47, 0.50, 0.48 and 0.45, respectively. These results again suggest that ERA5-Land and MSWEP capture a higher proportion of precipitation events but yield many false alarms, especially in winter. According to RRMSE, POD and CSI, precipitation products perform better in summer and worse in winter, which was also reported in Bangladesh [27] and the contiguous United States [35]. However, GSMAp, ERA5-Land and IMERG all show a significantly higher CC in winter than in summer by 0.13 on average.

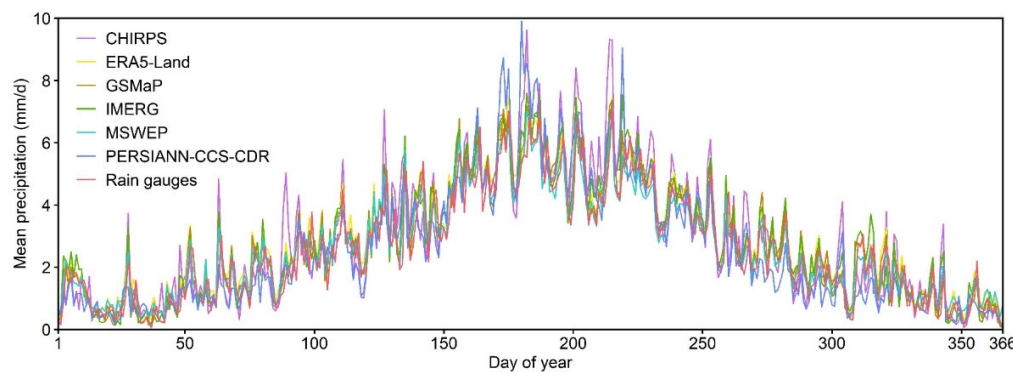


Figure 4. Mean time series of daily precipitation from rain gauges and six precipitation products during the year between 2015 and 2019.

Table 3. Mean values of CC, RRMSE, POD and CSI for different seasons between 2015 and 2019.

Product	Metric	Spring	Summer	Autumn	Winter
CHIRPS	CC	0.3	0.34	0.29	0.32
	RRMSE	4.31	3.17	4.71	6.15
	POD	0.33	0.44	0.28	0.25
	CSI	0.22	0.32	0.21	0.16
ERA5-Land	CC	0.45	0.47	0.52	0.62
	RRMSE	3.15	2.61	3.11	3.57
	POD	0.75	0.84	0.78	0.71
	CSI	0.43	0.49	0.44	0.38
GSMAp	CC	0.53	0.52	0.58	0.68
	RRMSE	2.97	2.55	3.04	3.35
	POD	0.74	0.81	0.75	0.66
	CSI	0.47	0.5	0.48	0.45
IMERG	CC	0.43	0.44	0.48	0.53
	RRMSE	3.45	2.88	3.58	4.89
	POD	0.61	0.72	0.59	0.4
	CSI	0.38	0.45	0.37	0.27
MSWEP	CC	0.5	0.5	0.55	0.53
	RRMSE	2.95	2.51	3.01	4.19
	POD	0.77	0.84	0.77	0.69
	CSI	0.44	0.5	0.45	0.39
PERSIANN-CCS-CDR	CC	0.25	0.25	0.25	0.2
	RRMSE	3.79	3.43	4.12	5.47
	POD	0.44	0.56	0.34	0.24
	CSI	0.25	0.35	0.22	0.14

3.2. Performance of Precipitation Products in Different Regions

3.2.1. Average Accuracy of Precipitation Products

Figure 7 provides four quantitative metrics of each precipitation product in the nine regions. Precipitation products have the highest CC in R₇ (0.50), higher CC in R₉, R₈, R₁, R₄ and R₃ (0.41–0.45), lower CC in R₅ and R₆ (0.35–0.36) and the lowest CC in R₂ (0.29). This indicates that the capability of capturing changes in the daily precipitation rate is higher in the eastern region than in the western region. As indicated by other studies [56,72], the poor performance of the products in R₅ and R₆ is likely due to the effects of snow surfaces and rugged topography, respectively. The CC yielded from PERSIANN-CCS-CDR is the lowest in each region, followed by CHIRPS. ERA5-Land has the highest CC in R₂ (0.43) and R₅ (0.48), and MSWEP has the highest CC in R₄ (0.54). In addition to the above regions, GSMAp has the highest CC, which suggests that GSMAp is optimal in the eastern region and the northeastern region. The nine regions in decreasing order of RRMSE are R₂, R₈, R₁, R₃, R₄, R₅, R₆, R₉ and R₇. R₂ has much higher RRMSE values than the other regions with a mean value of 6.05, and GSMAp and MSWEP, which perform very well in other regions, have RRMSE values of 6.49 and 6.41, respectively. In the other regions, the RRMSE values of ERA5-Land, GSMAp and MSWEP are almost the same and small. Based on RRMSE, CHIRPS and PERSIANN-CCS-CDR perform worse than the other four precipitation products in most regions. The POD and CSI of the six precipitation products indicate a geographic variation in precipitation detection capability, which decreases in the order of R₇, R₉, R₅, R₆, R₃, R₄, R₁, R₈ and R₂. The precipitation detection capability of each product ranks consistently among regions, with GSMAp having the best precipitation detection capability overall, followed by MSWEP and ERA5-Land. The precipitation products, except CHIRPS, tend to have false alarms for precipitation in all regions, which is particularly serious in R₂. Overall, precipitation products perform better in the eastern region, where the proportion of light rain is relatively low, because of their weak estimation of light rain (Section 3.1.2.).

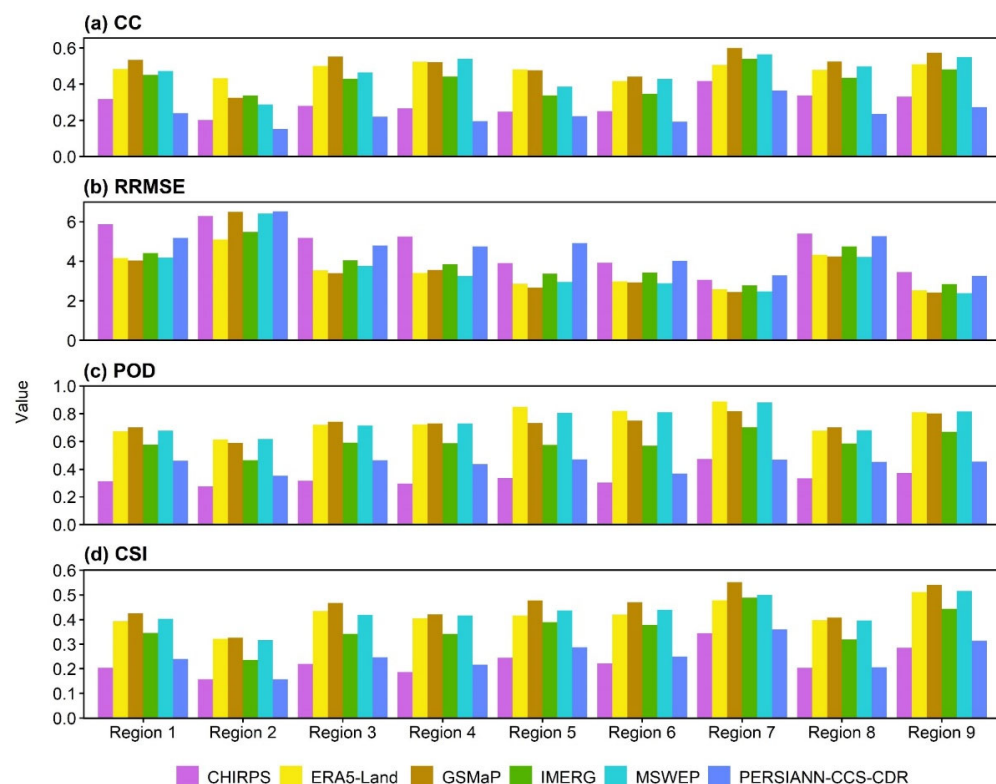


Figure 5. Mean values of (a) CC, (b) RRMSE, (c) POD and (d) CSI in the nine regions between 2015 and 2019.

3.2.2. Performance of Precipitation Products for Different Precipitation Levels

The PDFs in the nine regions are given in Figure 6. There are significant regional differences in the estimation of PDF among precipitation products, and the errors mainly exist in the estimation of no rain and light rain. The mean absolute error (MAE) can quantify the overall classification accuracy of the products, which is the absolute average of the biases of multiple precipitation levels. In general, precipitation products perform better in R₁, R₂ and R₈, with an MAE of less than 5%. In R₁, GSMAp underestimates no rain by 6.11% and overestimates light rain by 5.89%, with an MAE of 2.51%, which is the best product. CHIRPS has a bias of less than 2% for each category in R₂, making it the most accurate product in this region (MAE is 0.71%). CHIRPS also has the smallest MAE in R₄ and R₈, with values of 2.70% and 2.54%, respectively. Both GSMAp and PERSIANN-CCS-CDR perform well in R₃, with MAEs of 3.10% and 3.16%, respectively. In other regions, including R₅, R₆, R₇ and R₉, most precipitation products have challenges in estimating the PDF of daily precipitation rate, with mean MAEs of 6.83%, 7.87%, 7.86% and 6.41%, respectively. In contrast, PERSIANN-CCS-CDR has relatively good performance in R₅ and R₉, with MAEs of 2.71% and 3.56%, respectively, while IMERG performs best in R₆ and R₇, with MAEs of 1.87% and 3.13%, respectively.

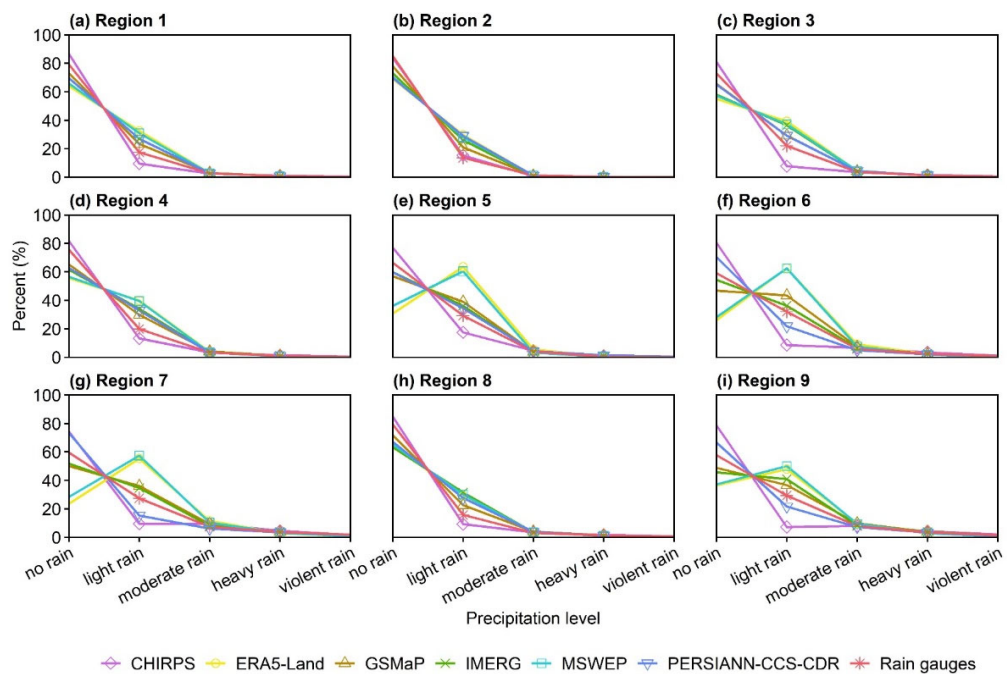


Figure 6. Probability density function of the daily precipitation rate of rain gauges and six precipitation products in different regions (a–i) between 2015 and 2019.

The statistical metrics for five precipitation levels in the nine regions are provided in Figure 7. Overall, precipitation products perform better in the western region than in the eastern region in terms of both light rain and moderate rain. However, they appear to have better performance in the eastern region for heavy rain and violent rain. In R₁, GSMAp is the best product for moderate, heavy and violent rain. For light rain, GSMAp has higher CC (0.29) and CSI (0.36) values, but its RRMSE (2.46) value is slightly higher than that of MSWEP (2.25), and its POD (0.62) value is lower than that of ERA5-Land (0.69) and MSWEP (0.69). ERA5-Land has higher CC and POD values, 0.27 and 0.72, respectively, for light rain in R₂, and MSWEP and GSMAp have the best RRMSE (1.75) and CSI (0.32) values, respectively. GSMAp performs best for moderate rain, with a CC of 0.18, RRMSE of 0.76, POD of 0.24 and CSI of 0.15. It also has relatively good RRMSE, POD and CSI values of 0.75, 0.13 and 0.08, respectively, for heavy rain. GSMAp performs relatively well at all precipitation levels in R₃, while it has a lower POD value of 0.65 than ERA5-Land (0.71) and

MSWEP (0.70) for light rain and a lower CC value of 0.27 than MSWEP (0.30) for violent rain. In R₄, MSWEP has better CC (0.27), RRMSE (2.00) and POD (0.74) values for light rain, and GSMAp performs better in terms of CSI values (0.35). GSMAp is the best product for moderate rain and heavy rain, with a slightly higher RRMSE of 0.74 than MSWEP (0.72) for moderate rain. Based on RRMSE and CSI values, GSMAp performs better than the others for violent rain, with values of 0.75 and 0.08, respectively, while ERA5-Land and CHIRPS perform better based on CC (0.23) and POD (0.13) values. GSMAp has a higher CC and CSI for light rain and moderate rain in R₅. In terms of RRMSE and POD, MSWEP and ERA5-Land are better for light rain and moderate rain, respectively. For heavy rain, ERA5-Land has the best CC and RRMSE, with values of 0.11 and 0.70, respectively, and GSMAp has a higher POD and CSI, with values of 0.07 and 0.05, respectively. Precipitation products perform similarly in the other four regions (R₆, R₇, R₈ and R₉): At the light rain level, GSMAp tends to have higher CC and CSI values, while MSWEP has better performance based on RRMSE and POD. In both R₆ and R₇, GSMAp, MSWEP and ERA5-Land perform better according to CSI, RRMSE and POD values for moderate rain, respectively. In terms of CC, MSWEP and GSMAp are better in R₆ and R₇, respectively. In R₈ and R₉, GSMAp has a higher CC, POD and CSI for moderate rain, while MSWEP has a smaller RRMSE. GSMAp is the best product for both heavy and violent rain, but it has lower POD values than IMERG in R₈ and R₉.

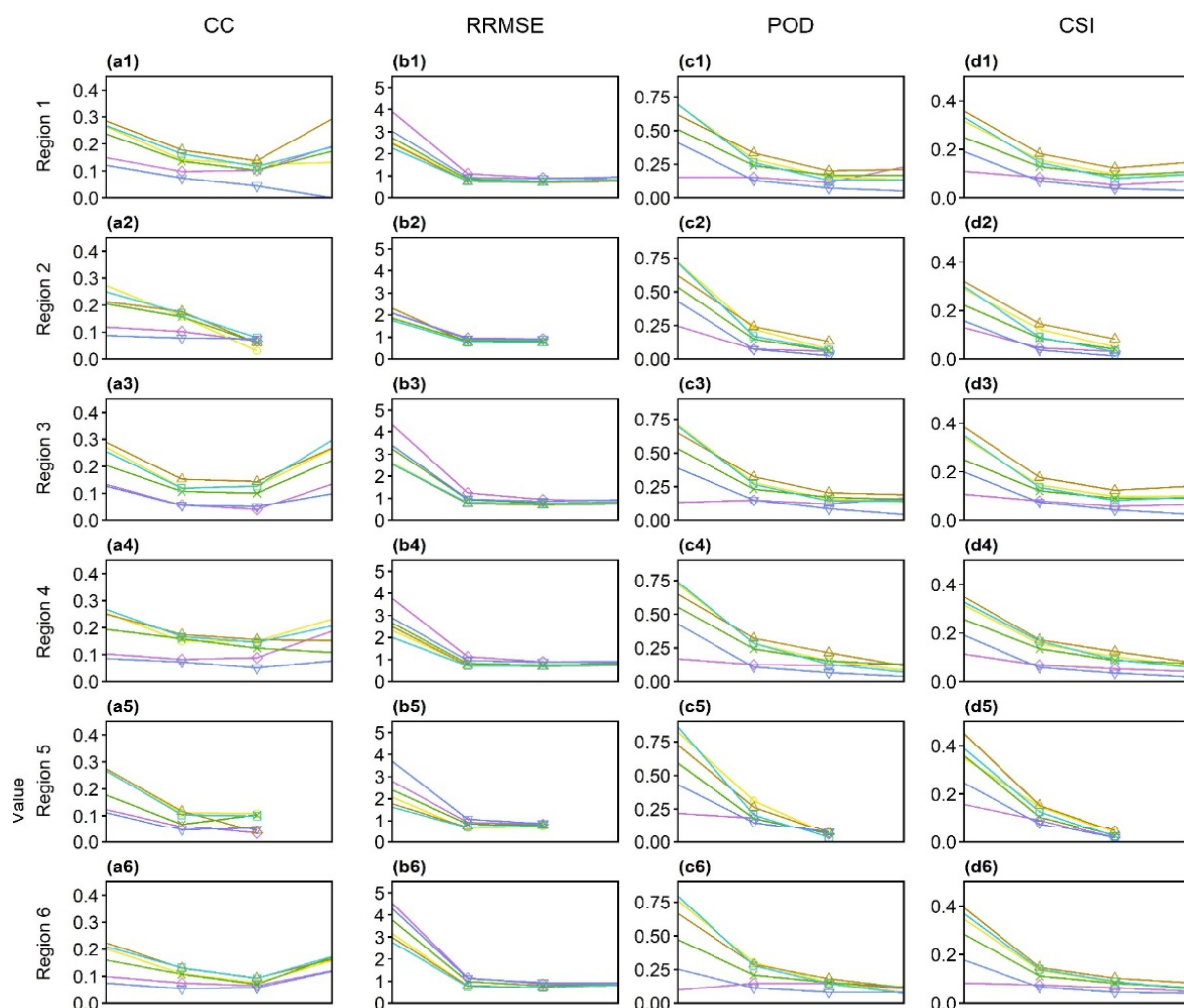


Figure 7. Cont.

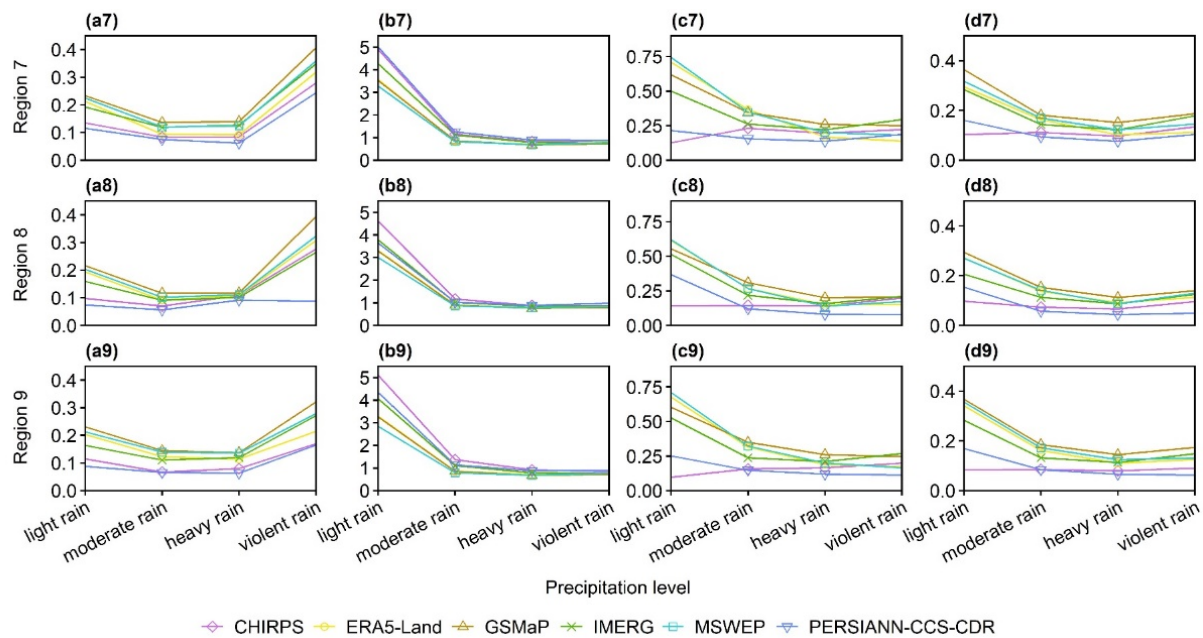


Figure 7. Mean values of four statistical metrics of precipitation products at four precipitation levels in different regions between 2015 and 2019. From left to right: (a1–a9) CC, (b1–b9) RRMSE, (c1–c9) POD and (d1–d9) CSI. Violent rain is not counted in R_2 and R_5 due to the low frequency of events.

3.2.3. Performance of Precipitation Products in Time Series

Figure 8 shows the time series of daily precipitation of rain gauges and six products in the nine regions. It is evident that the amount and pattern of precipitation vary significantly between the nine regions of mainland China. R_2 is the driest region with low daily precipitation throughout the year, and small biases are found between the precipitation products and real observations. Most products show significant overestimation in R_5 , especially in the rainy season. It is possible that the satellite sensors are affected by the snow cover on the Tibetan Plateau [72]. R_7 and R_9 are the regions with the most abundant precipitation; although the differences between the products and observations are large, the RRMSE values are very low, with values of 2.77 and 2.81, respectively (Figure 7). In addition, the performance of some precipitation products varies greatly among regions. For example, MSWEP always overestimates precipitation from the 330th day to the 40th day of the following year in relatively cold regions, including R_1 , R_2 , R_3 and R_5 . PERSIANN-CCS-CDR exhibits overestimation in rainy months in R_2 , R_5 , R_6 and R_7 . As shown in Figure 8, CHIRPS frequently overestimates precipitation during the wet season in the northern region, including R_1 , R_3 , R_4 and R_8 , yet the overestimation mainly occurs in the wet–dry transition season in the southern region, including R_6 , R_7 and R_9 . For CHIRPS, a recent study has shown that CHIRPS significantly overestimates precipitation from 20°N to 30°N mainly in spring and summer, especially in the southern region [73]. The overestimation that occurred in the southern region by CHIRPS may be due to the differences with regard to station type and numbers in southeastern China [73].

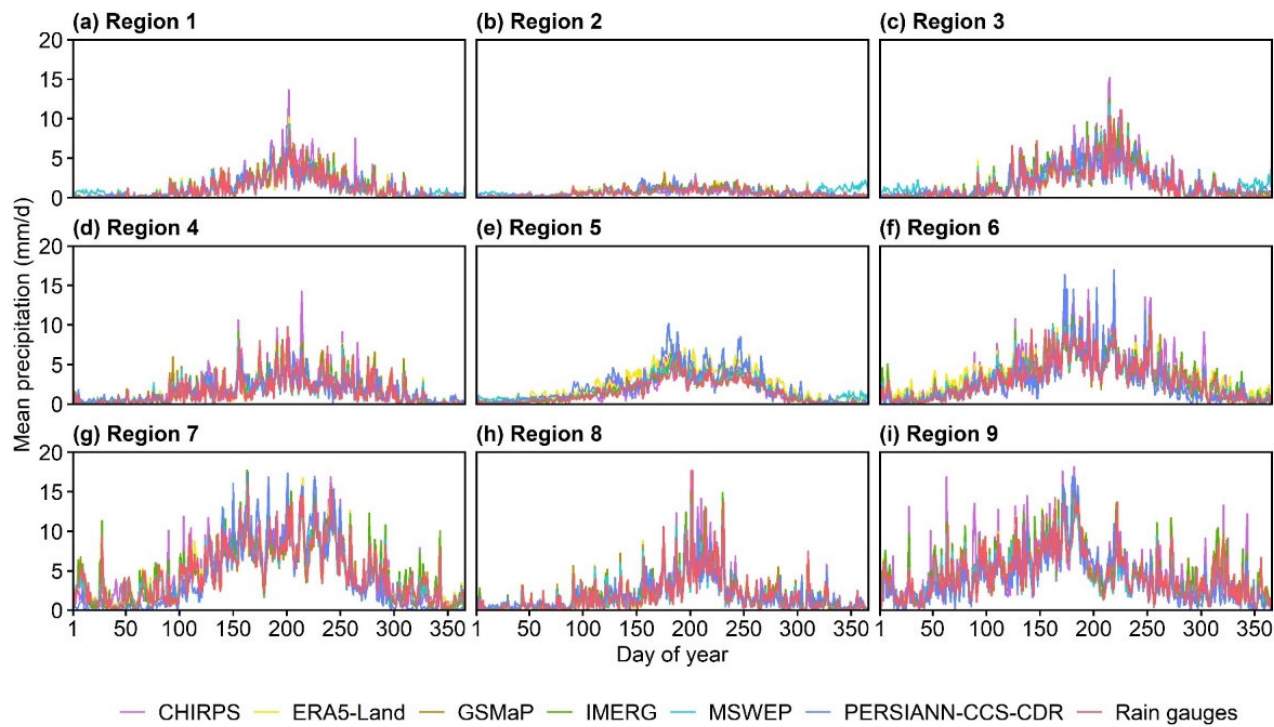


Figure 8. Mean time series of daily precipitation of rain gauges and six products during the year in different regions (a–i) between 2015 and 2019.

3.2.4. Performance of Precipitation Products in Different Seasons

Figure 9 shows the spatial distribution of CC values across the seasons. In spring, GSMAp and MSWEP have better performance, with their CC values ranging from 0.37 to 0.63 and from 0.36 to 0.59, respectively. Specifically, GSMAp has the highest CC in R₃, R₆, R₇, R₈ and R₉, with values of 0.63, 0.38, 0.56, 0.52 and 0.51, respectively, while MSWEP performs better in R₁ (0.59) and R₄ (0.53), and ERA5-Land performs better in R₂ (0.41) and R₅ (0.46). In general, most precipitation products are more accurate in the northern region, with mean CC values of 0.48 and 0.45, respectively. MSWEP and GSMAp also perform better in most regions in summer, with mean CC values of 0.47 and 0.46, respectively. GSMAp has the highest CC in all regions, except R₂, where MSWEP has a significantly higher CC value of 0.45 than GSMAp (0.28). The mean CC values of R₇ and R₉ in summer are 0.48 and 0.46, respectively, which are higher than those of other regions. In autumn, GSMAp performs best, with a mean CC value of 0.54, which has the highest CC in all regions except R₂ and R₅, while ERA5-Land has a higher accuracy, with a CC value of 0.46 in those two regions. In winter, GSMAp and ERA5-Land have a significant advantage over the other products, with mean CC values of 0.57 and 0.54, respectively. ERA5-Land still performs well in R₂ and R₅, with CC values of 0.49 and 0.48, respectively. MSWEP has the highest CC value of 0.54 in R₄, and the best product in the other regions is GSMAp. The mean CC value of products is higher in R₇ than in the other regions. Furthermore, there are four regions (R₂, R₄, R₅ and R₈) where the CC values of products are higher in autumn and in the southern region with higher CC values in winter.

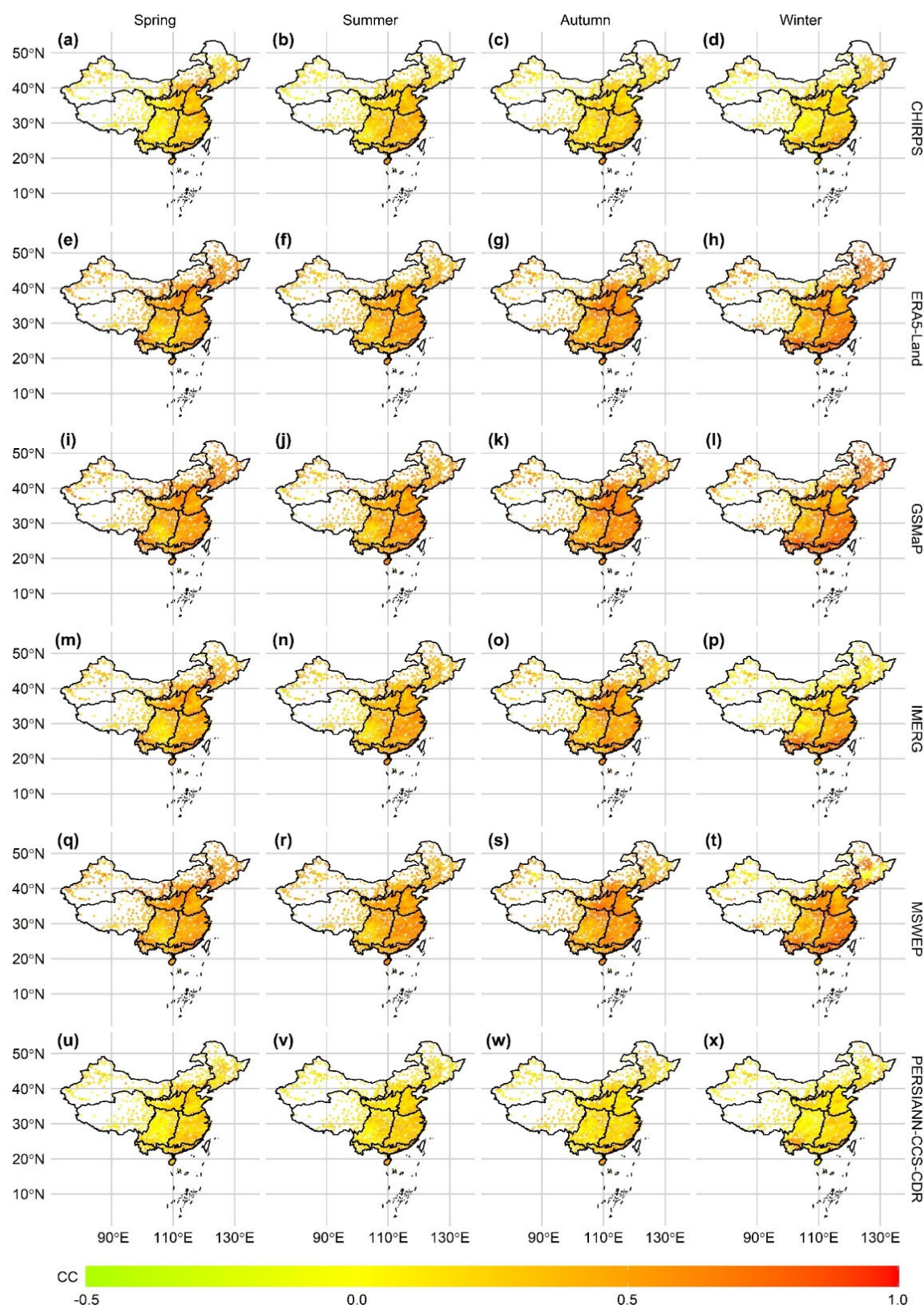


Figure 9. Distribution of CC values of six products for different seasons between 2015 and 2019. From top to bottom: (a–d) CHIRPS, (e–h) ERA5-Land, (i–l) GSMAp, (m–p) IMERG, (q–t) MSWEP and (u–x) PERSIANN-CCS-CDR.

The spatial distribution of RRMSE is displayed in Figure 10. In spring, MSWEP has a smaller mean RRMSE value (3.31) in the nine regions than the other products and performs best in six regions (R_1 , R_2 , R_4 , R_5 , R_8 and R_9), with mean RRMSE values of 3.92, 5.43, 3.15, 2.62, 3.91 and 2.12, respectively. In the other three regions (R_3 , R_6 and R_7), the RRMSE values of GSMAp are smaller, with values of 3.18, 2.84 and 2.51, respectively. MSWEP also performs best in summer, with a mean RRMSE value of 2.57 in the nine regions. Except for R_3 and R_7 , MSWEP has the smallest RRMSE values in all regions in summer. MSWEP and GSMAp perform better than the other products in autumn and winter, with mean RRMSE values in the nine regions of 3.16 and 4.49, respectively. MSWEP performs best in R_1 , R_3 , R_4 , R_5 , R_6 , R_7 and R_8 in autumn, with RRMSE values of 3.21, 3.36, 2.50, 2.46, 2.58, 2.76 and 3.34, respectively. GSMAp is better in R_1 , R_3 , R_5 , R_6 , R_7 , R_8 and R_9 in winter, with RRMSE values of 5.48, 3.46, 6.95, 3.39, 3.07, 5.09 and 2.06, respectively. Overall, the RRMSE values in R_7 and R_9 are smaller in each season. Additionally, precipitation products perform better in summer in all regions except R_9 , where RRMSE is slightly smaller in spring than in summer.

Figures 11 and 12 provide the distribution of POD and CSI of the precipitation products, respectively. In each season, the performance of the precipitation products in R_7 and R_9 is better than that in other regions. ERA5-Land has a higher mean POD, and GSMAp has a higher mean CSI in each season. More specifically, GSMAp has higher POD values in R_1 (0.63), R_3 (0.71), R_4 (0.70) and R_8 (0.65) in spring; in R_1 (0.78), R_2 (0.63), R_3 (0.82) and R_8 (0.75) in summer; in R_1 (0.66), R_3 (0.69), R_4 (0.76), R_8 (0.70) and R_9 (0.79) in autumn; and in R_8 (0.58) in winter. The POD values of MSWEP in R_6 (0.77) and R_9 (0.83) in spring, in R_4 (0.76) and R_6 (0.90) in summer, in R_2 (0.63) in autumn, and in R_1 (0.49) and R_9 (0.76) in winter are higher than those of the other products. For other situations, the POD values of ERA5-Land are the largest. On the other hand, GSMAp performs best in terms of CSI for all regions in each season, except for R_1 in spring and R_1 and R_2 in summer, where MSWEP performs better. Except for R_2 , the precipitation detection capability of products tends to be better in summer. The performance of the products in R_2 is slightly better in spring than in summer.

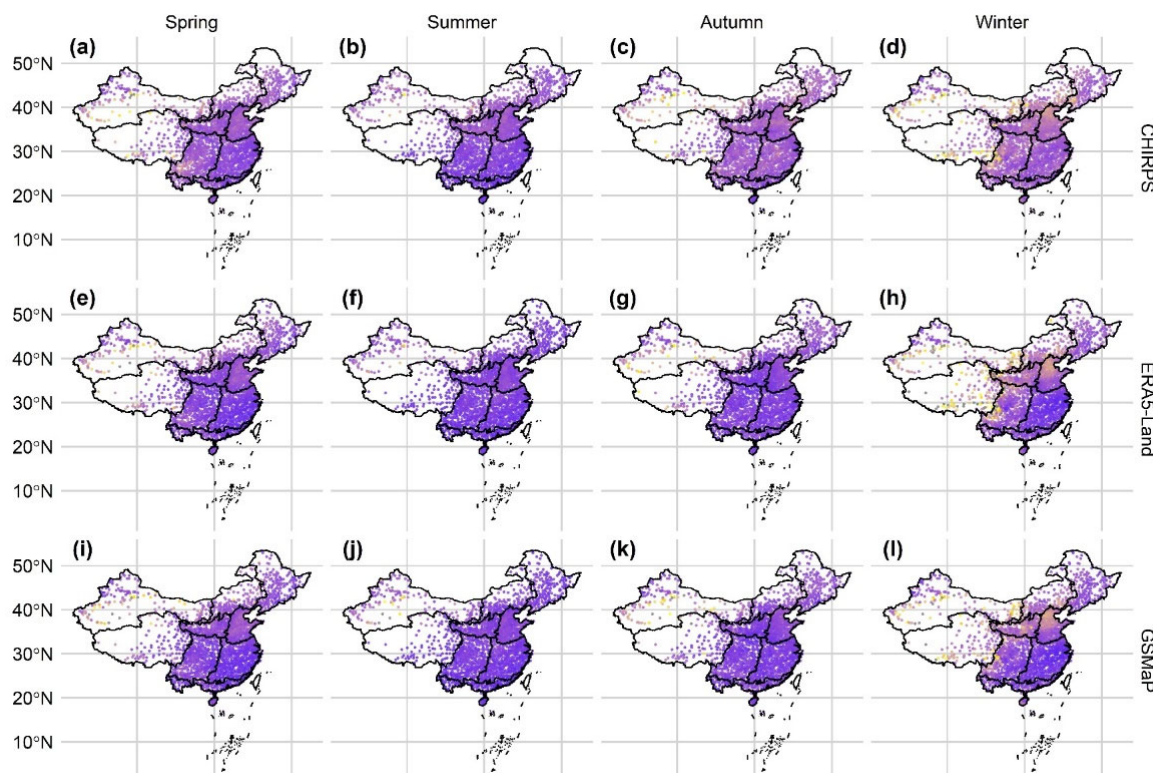


Figure 10. Cont.

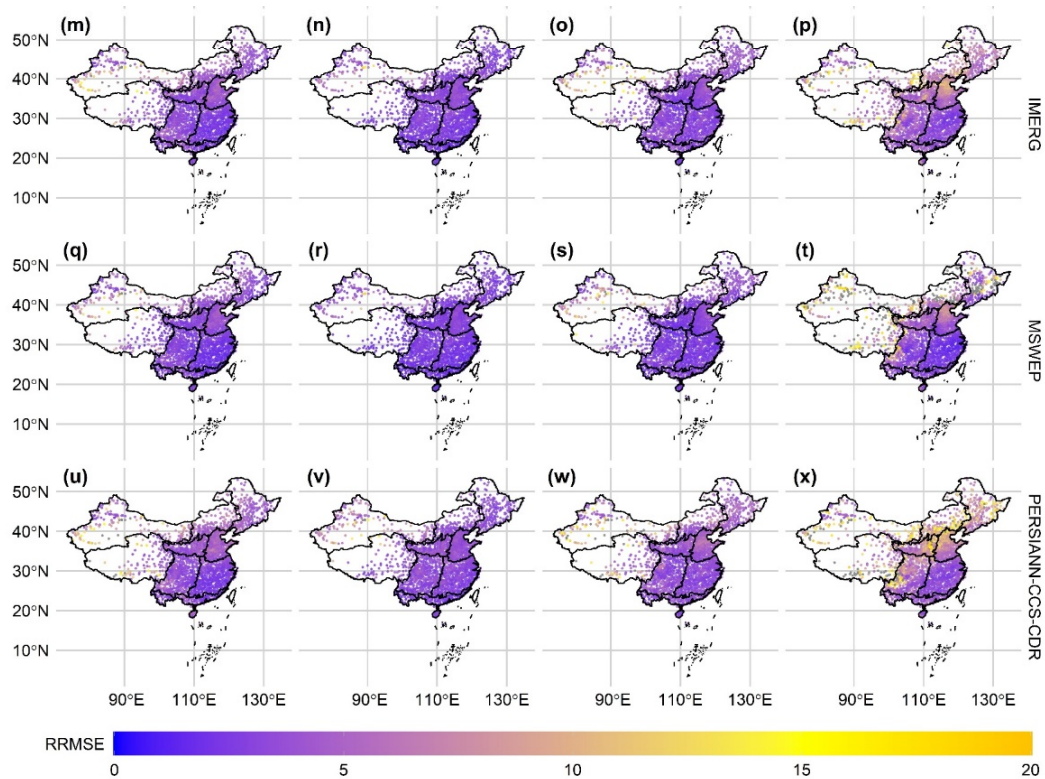


Figure 10. Distribution of RRMSE values of six products for different seasons between 2015 and 2019. From top to bottom: (a–d) CHIRPS, (e–h) ERA5-Land, (i–l) GSMAp, (m–p) IMERG, (q–t) MSWEP and (u–x) PERSIANN-CCS-CDR.

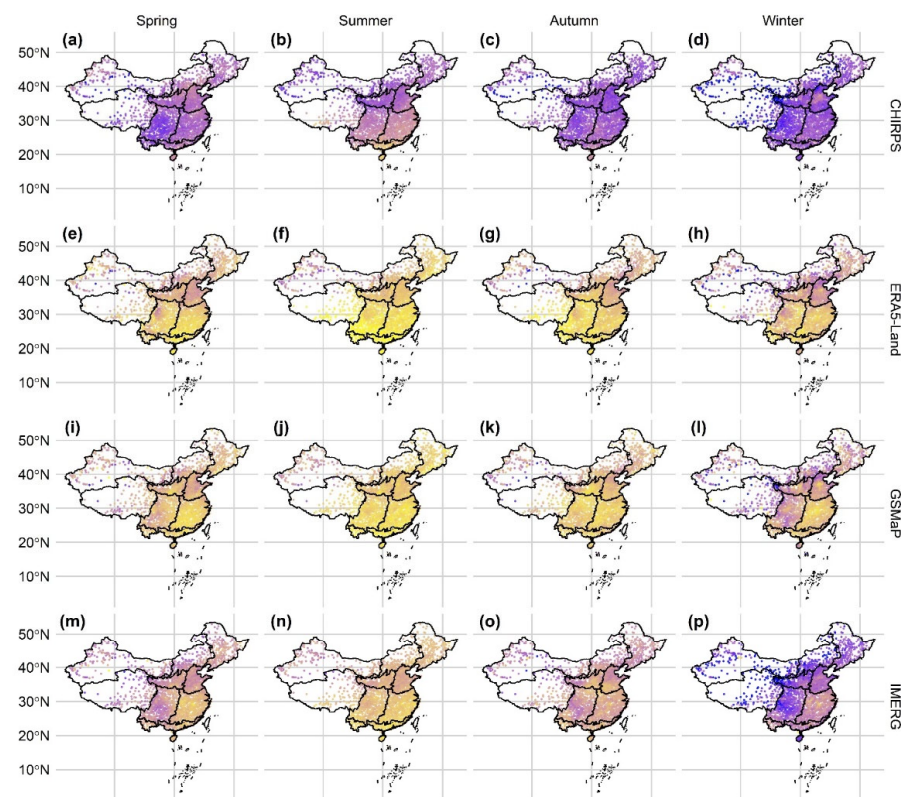


Figure 11. Cont.

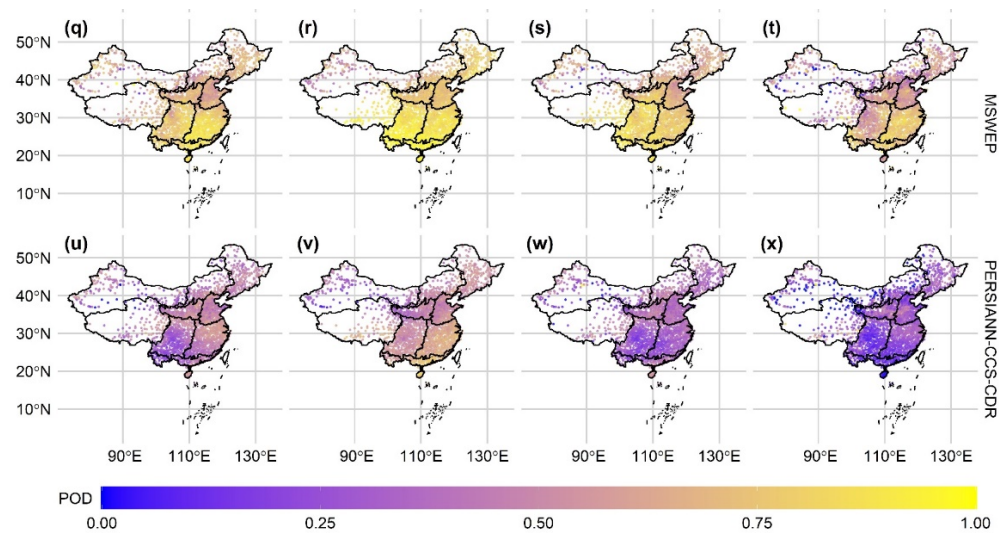


Figure 11. Distribution of POD values of six products for different seasons between 2015 and 2019. From top to bottom: (a–d) CHIRPS, (e–h) ERA5-Land, (i–l) GSMAp, (m–p) IMERG, (q–t) MSWEP and (u–x) PERSIANN-CCS-CDR.

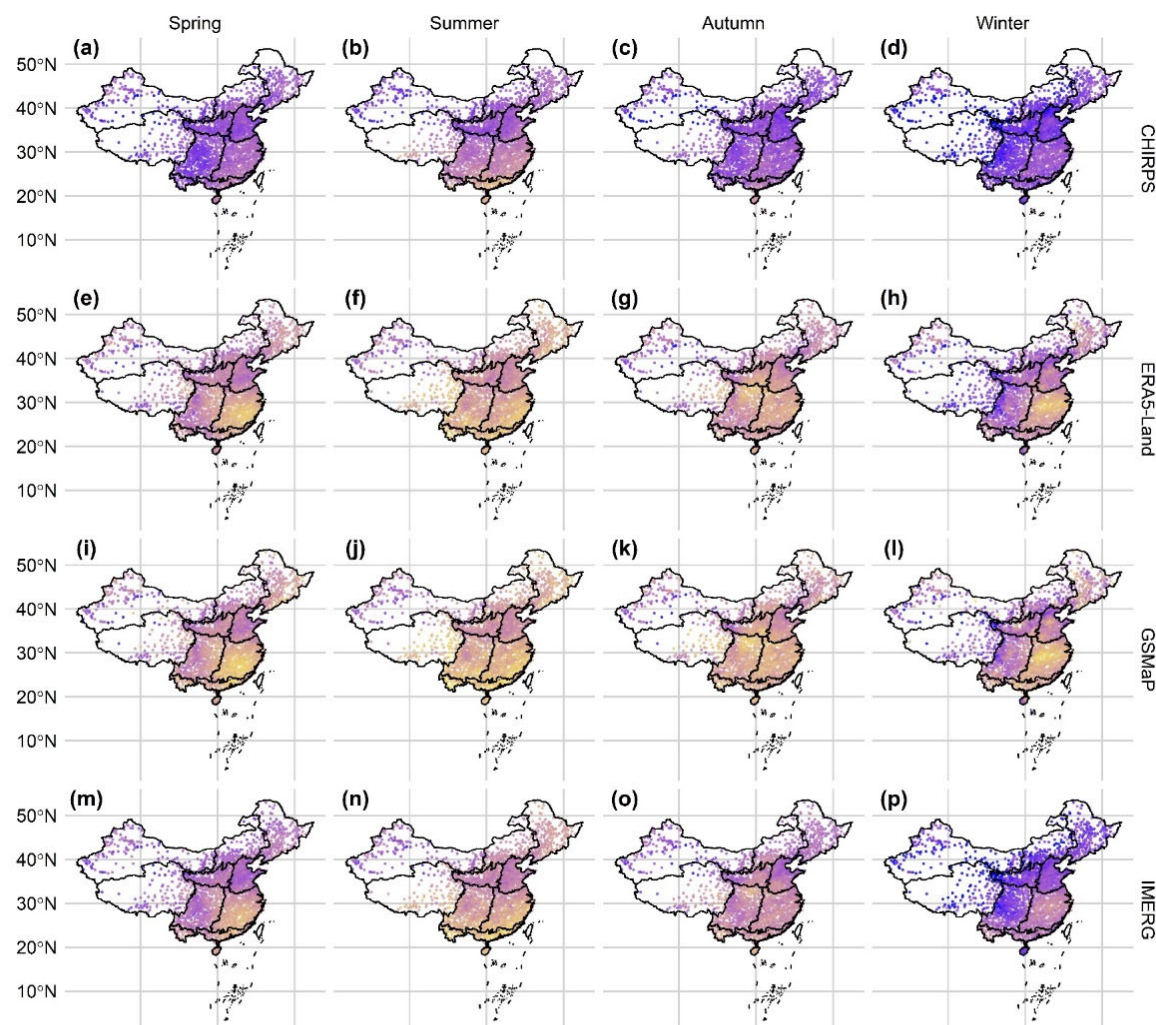


Figure 12. Cont.

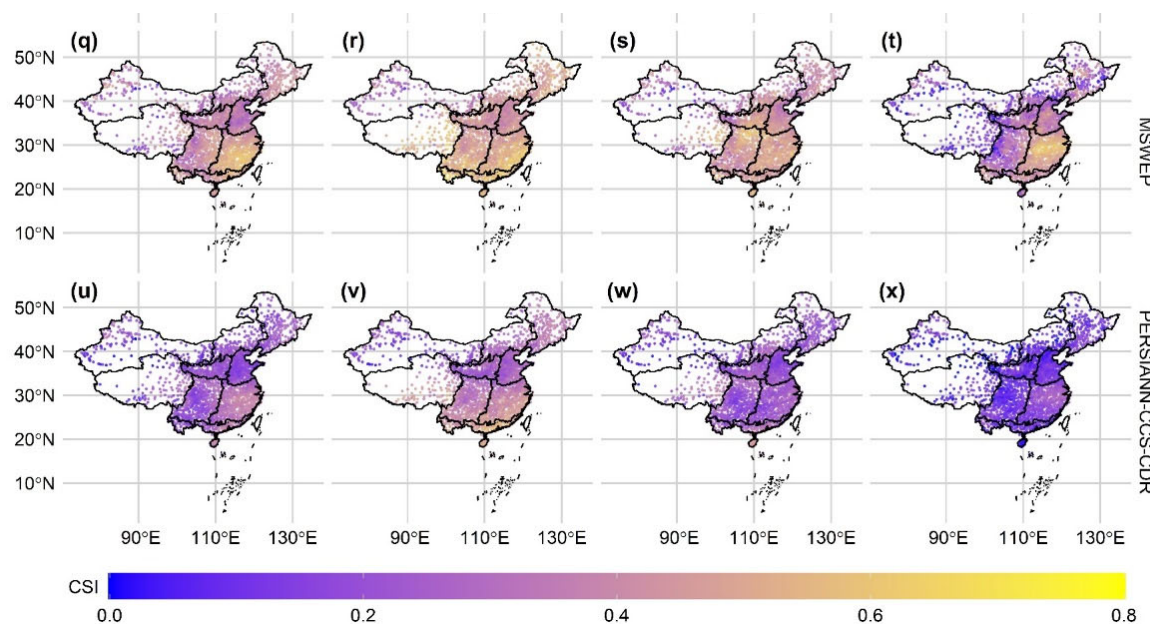


Figure 12. Distribution of the CSI values of six products for different seasons between 2015 and 2019. From top to bottom: (a–d) CHIRPS, (e–h) ERA5-Land, (i–l) GSMAp, (m–p) IMERG, (q–t) MSWEP and (u–x) PERSIANN-CCS-CDR.

4. Discussion

Many researchers have recognized the importance of evaluating precipitation products for various studies and have conducted numerous studies to evaluate the performance of single or multiple precipitation products in different areas [29,57,61]. However, these studies often suffer from the following major problems. First, many previous studies focus on very few precipitation products. For example, they compared IMERG and GSMAp [28] or evaluated the progressiveness of the gauge-adjusted version of GSMAp [30], which is insufficient for obtaining the relatively optimal product for specific applications. Conclusions drawn from comparing all or most of the available prominent high-quality datasets would provide more meaningful selection guidance for product selection. Second, many evaluation studies are conducted at multiple temporal scales [34,56], which leads to many important features; however, the comparison at a single scale cannot be detected in detail due to the space limitation in the paper. Specifically, daily precipitation products are critically important in agriculture, vegetation and ecology [42,43], but previous attempts are still insufficient. Furthermore, previous evaluation studies divided the study area mostly based on topography, watershed, or even administrative division, which were very useful for certain studies. However, performance of different precipitation datasets in different agriculture regions are also of special interest, as many regional agricultural studies are often conducted in a specific agricultural region [44–47]. To our knowledge, no studies have been conducted specifically to evaluate daily precipitation products in different agriculture regions in China, which would be of crucial importance for better agricultural applications.

To address these shortcomings, this study was conducted to provide a comprehensive evaluation and comparison of six high-quality and promising products at a daily scale across different agricultural regions of mainland China to facilitate related regional and local applications. The results show that GSMAp has the best overall performance compared with other products, especially in detecting heavy and violent rain, which is mainly attributed to its advanced sensors and retrieval algorithms [53]. However, the estimation of light rain is still the main difficulty of GSMAp, although it has benefited greatly from the GMI sensor in detecting light rain [70]. In this study, GSMAp outperforms IMERG most of the time, which is consistent with previous findings [41,74]. According to further research, this may be due to the daily scale adjustment of GSMAp, a method that may also be able to be used

to improve other products [74]. The RRMSE values of MSWEP tend to be smaller than those of the other products in most seasons and regions, which was also confirmed by other studies [36,65]. However, MSWEP overcorrects the PDF, thus obtaining the best statistical performance to the extent that it has poor classification accuracy for precipitation levels, especially for light rain [65]. This study and a study by Gao et al. [75] both demonstrate that ERA5-Land has high POD values and a large number of false alarms.

The results obtained from this study are important for researchers to select suitable daily precipitation data for specific applications throughout mainland China. For example, detecting the precipitation ability of different products at different precipitation thresholds is fundamental to a wide variety of applications, including developing early warning systems and disaster management strategies [76,77]. In addition, a large number of studies are focusing on the influence of daily precipitation on various crops or vegetation [78,79]. Daily precipitation products can also play a major role in agricultural disaster preparedness and crop environmental restoration [80]. Furthermore, integrating high-quality precipitation data into hydrological models or land-surface models could result in reliable output, especially for applications that are sensitive to precipitation change, which places a particular emphasis on the identification of the relatively optimal products for the specific region [81].

There are still some methodological uncertainties in this study, including the scale mismatch issue between the rain gauges and the precipitation products, the statistical uncertainty due to the uneven density of the station distribution, and the differences in the definition of day between rain gauges and precipitation products. These issues are very common in evaluation studies of precipitation products and affect the evaluation results yet have not been addressed to our knowledge [34,51,65,73,75]. The prevailing approaches were adopted to avoid introducing further uncertainties in this study, as explained in Section 2.3.1. How to mitigate the impact of these uncertainties on the evaluation is an important issue that needs to be addressed in the future.

In addition, uncertainty in the satellite-based precipitation products may also affect the evaluation and comparison studies. For example, El Niño–Southern Oscillation (ENSO) is one of the most important factors affecting global precipitation [82] and has a strong influence on the annual variation of precipitation in China [83]. Many studies have found that precipitation anomalies due to the ENSO events are often under- or overestimated in satellite precipitation products [84–86]. Moreover, the performance of different precipitation products under the influence of various ENSO types is likely to be different due to their different retrieval algorithms [86,87]. Therefore, the results of evaluation studies, including the measurement of error distributions and the selection of optimal products, may also be influenced by ENSO. Further comparison should be conducted by taking into account the factors of annual variation in rainfall production.

5. Conclusions

In this study, six high-resolution daily precipitation products, including CHIRPS, ERA5-Land, GSMAp, IMERG, MSWEP and PERSIANN-CCS-CDR, were evaluated and compared between 2015 and 2019 throughout mainland China. The main conclusions are as follows.

- (1) In general, GSMAp is the best precipitation product, especially in terms of CC and CSI, and MSWEP tends to have the smallest RRMSE values. In addition, ERA5-Land and MSWEP can detect a greater proportion of precipitation events most of the time.
- (2) In terms of the PDF of daily precipitation rate, the product with the highest accuracy in different regions are not the same. Based on statistical metrics, GSMAp is relatively better at all precipitation levels, especially for heavy and violent rain, while MSWEP has smaller RRMSE values than GSMAp for light and moderate rain.
- (3) Considering the overall performance of the precipitation products, each agricultural region has one or two optimal precipitation products. Specifically, GSMAp is the best product in the Inner Mongolia Plateau, the Northeast Plain, the Huang-Huaihai Plain and the Middle and Lower Yangtze River. In addition, ERA5-Land and MSWEP are

performed better in the Gan-Xin Desert Plateau and the Loess Plateau, respectively. In the Qinghai-Tibet Plateau region, GSMAp and ERA5-Land perform the best in terms of different errors metrics. In the Sichuan Basin, the Yunnan-Guizhou Plateau and the South China Tropical Crops Region, GSMAp and MSWEP perform similarly and better than other precipitation products.

- (4) MSWEP performs better than others at capturing the characteristics of the daily precipitation time series, with smaller average deviations and fewer extreme errors. GSMAp performs the best in each season, while GSMAp has higher RRMSE values than MSWEP and smaller POD values than both ERA5-Land and MSWEP. Generally, all precipitation products perform better in summer and worse in winter based on error measurements and precipitation detection capability, and they perform better in the eastern region.

We analyzed the performance of six high-resolution precipitation products in nine regions from different aspects and identified the optimal product in each region. The findings provide the optimal precipitation product for each region, which is important for local studies. In addition, our results could facilitate further product improvement work or the production of new multisource fusion precipitation products.

Author Contributions: Conceptualization, N.Z.; methodology, X.W.; validation, X.W.; formal analysis, X.W.; investigation, X.W.; resources, N.Z.; data curation, X.W.; writing—original draft preparation, X.W.; writing—review and editing, N.Z.; visualization, X.W.; supervision, N.Z.; project administration, N.Z.; funding acquisition, N.Z. All authors have read and agreed to the published version of the manuscript.

Funding: This research was funded by the National Natural Science Foundation of China, grant number 42071374, 42293270 and 41930647, and the Strategic Priority Research Program (A) of the Chinese Academy of Sciences, grant number XDA20030203.

Data Availability Statement: The precipitation products used in this study were accessed from the following freely available sources: (i) CHIRPS (<https://data.chc.ucsb.edu/products/CHIRPS-2.0/>), accessed on 22 June 2022), (ii) GSMAp (<https://gportal.jaxa.jp/>), accessed on 2 July 2022), (iii) IMERG (https://gpm1.gesdisc.eosdis.nasa.gov/opendap/GPM_L3/GPM_3IMERGDF.06/), accessed on 2 July 2022), (iv) MSWEP (<http://www.globo2o.org/>), accessed on 4 July 2022), (v) PERSIANN-CCS-CDR (<http://persiann.eng.uci.edu/CHRSdata/PCCSCDR/>), accessed on 5 July 2022), and (vi) ERA5-Land (<https://cds.climate.copernicus.eu/cdsapp#!/dataset/reanalysis-era5-land/>), accessed on 12 July 2022). Due to privacy and ethical concerns, the rain gauge data from CMA cannot be made available.

Acknowledgments: We are very grateful to the editors and reviewers who significantly contributed to the improvement of this paper.

Conflicts of Interest: The authors declare no conflict of interest.

References

- Qi, Z.; Zhou, X.; Tian, L.; Zhang, H.; Cai, L.; Tang, F. Distribution of mycotoxin-producing fungi across major rice production areas of China. *Food Control* **2022**, *134*, 108572. [[CrossRef](#)]
- Tuo, Y.; Marcolini, G.; Disse, M.; Chiogna, G. A multi-objective approach to improve SWAT model calibration in alpine catchments. *J. Hydrol.* **2018**, *559*, 347–360. [[CrossRef](#)]
- Xiang, Y.; Li, Y.; Liu, Y.; Zhang, S.; Yue, X.; Yao, B.; Xue, J.; Lv, W.; Zhang, L.; Xu, X.; et al. Factors shaping soil organic carbon stocks in grass covered orchards across China: A meta-analysis. *Sci. Total Environ.* **2022**, *807*, 150632. [[CrossRef](#)] [[PubMed](#)]
- Chen, J.; Chung, C. Representation of global precipitation anomalies using four major climate patterns. *Sci. China Technol. Sci.* **2015**, *58*, 927–934. [[CrossRef](#)]
- Wu, H.; Yang, Q.; Liu, J.; Wang, G. A spatiotemporal deep fusion model for merging satellite and gauge precipitation in China. *J. Hydrol.* **2020**, *584*, 124664. [[CrossRef](#)]
- Herold, N.; Alexander, L.V.; Donat, M.G.; Contractor, S.; Becker, A. How much does it rain over land? *Geophys. Res. Lett.* **2016**, *43*, 341–348. [[CrossRef](#)]
- Prein, A.F.; Gobiet, A. Impacts of uncertainties in European gridded precipitation observations on regional climate analysis. *Int. J. Climatol.* **2017**, *37*, 305–327. [[CrossRef](#)]
- Liu, Z.; Liu, Y.; Wang, S.; Yang, X.; Wang, L.; Baig, M.H.A.; Chi, W.; Wang, Z. Evaluation of Spatial and Temporal Performances of ERA-Interim Precipitation and Temperature in Mainland China. *J. Climate* **2018**, *31*, 4347–4365. [[CrossRef](#)]

9. Yang, T.; Li, Q.; Chen, X.; De Maeyer, P.; Yan, X.; Liu, Y.; Zhao, T.; Li, L. Spatiotemporal variability of the precipitation concentration and diversity in Central Asia. *Atmos. Res.* **2020**, *241*, 104954. [[CrossRef](#)]
10. Jin, H.; Chen, X.; Wu, P.; Song, C.; Xia, W. Evaluation of spatial-temporal distribution of precipitation in mainland China by statistic and clustering methods. *Atmos. Res.* **2021**, *262*, 105772. [[CrossRef](#)]
11. Beck, H.E.; Wood, E.F.; McVicar, T.R.; Zambrano-Bigiarini, M.; Alvarez-Garreton, C.; Baez-Villanueva, O.M.; Sheffield, J.; Karger, D.N. Bias Correction of Global High-Resolution Precipitation Climatologies Using Streamflow Observations from 9372 Catchments. *J. Climate* **2020**, *33*, 1299–1315. [[CrossRef](#)]
12. Brunetti, M.; Maugeri, M.; Monti, F.; Nannia, T. Temperature and precipitation variability in Italy in the last two centuries from homogenised instrumental time series. *Int. J. Climatol.* **2006**, *26*, 345–381. [[CrossRef](#)]
13. Zambrano, F.; Wardlow, B.; Tadesse, T.; Lillo-Saavedra, M.; Lagos, O. Evaluating satellite-derived long-term historical precipitation datasets for drought monitoring in Chile. *Atmos. Res.* **2017**, *186*, 26–42. [[CrossRef](#)]
14. Markonis, Y.; Papalexiou, S.M.; Martinkova, M.; Hanel, M. Assessment of Water Cycle Intensification Over Land using a Multisource Global Gridded Precipitation DataSet. *J. Geophys. Res. D Atmos.* **2019**, *124*, 11175–11187. [[CrossRef](#)]
15. Funk, C.; Peterson, P.; Landsfeld, M.; Pedreros, D.; Verdin, J.; Shukla, S.; Husak, G.; Rowland, J.; Harrison, L.; Hoell, A.; et al. The climate hazards infrared precipitation with stations-a new environmental record for monitoring extremes. *Sci. Data* **2015**, *2*, 150066. [[CrossRef](#)]
16. Okamoto, K.; Ushio, T.; Iguchi, T.; Takahashi, N.; Iwanami, K. The global satellite mapping of precipitation (GSMP) project. In Proceedings of the 25th IEEE International Geoscience and Remote Sensing Symposium (IGARSS 2005), Seoul, Republic of Korea, 29 July 2005; pp. 3414–3416.
17. Huffman, G.J.; Bolvin, D.T.; Braithwaite, D.; Hsu, K.; Joyce, R.; Xie, P.; Yoo, S.-H. NASA global precipitation measurement (GPM) integrated multi-satellite retrievals for GPM (IMERG). In *Algorithm Theoretical Basis Document (ATBD) Version 06*; NASA: Washington, DC, USA, 2015.
18. Beck, H.E.; Wood, E.F.; Pan, M.; Fisher, C.K.; Miralles, D.G.; van Dijk, A.I.J.M.; McVicar, T.R.; Adler, R.F. MSWEP V2 Global 3-Hourly 0.1 degrees Precipitation: Methodology and Quantitative Assessment. *Bull. Amer. Meteor. Soc.* **2019**, *100*, 473–502. [[CrossRef](#)]
19. Sadeghi, M.; Nguyen, P.; Naeini, M.R.; Hsu, K.; Braithwaite, D.; Sorooshian, S. PERSIANN-CCS-CDR, a 3-hourly 0.04° global precipitation climate data record for heavy precipitation studies. *Sci. Data* **2021**, *8*, 157. [[CrossRef](#)]
20. Munoz-Sabater, J.; Dutra, E.; Agusti-Panareda, A.; Albergel, C.; Arduini, G.; Balsamo, G.; Boussetta, S.; Choulga, M.; Harrigan, S.; Hersbach, H.; et al. ERA5-Land: A state-of-the-art global reanalysis dataset for land applications. *Earth Syst. Sci. Data* **2021**, *13*, 4349–4383. [[CrossRef](#)]
21. Canedo-Rosso, C.; Hochrainer-Stigler, S.; Pflug, G.; Condori, B.; Berndtsson, R. Drought impact in the Bolivian Altiplano agriculture associated with the El Nino-Southern Oscillation using satellite imagery data. *Nat. Hazards Earth Syst. Sci.* **2021**, *21*, 995–1010. [[CrossRef](#)]
22. Bento, V.A.; Russo, A.; Dutra, E.; Ribeiro, A.F.S.; Gouveia, C.M.; Trigo, R.M. Persistence versus dynamical seasonal forecasts of cereal crop yields. *Sci. Rep.* **2022**, *12*, 7422. [[CrossRef](#)]
23. Ghaedamini, H.A.; Morid, S.; Nazemosadat, M.J.; Shamsoddini, A.; Moghadam, H.S. Validation of the CHIRPS and CPC-Unified Products for Estimating Extreme Daily Precipitation Over Southwestern Iran. *Theor. Appl. Climatol.* **2021**, *146*, 1207–1225. [[CrossRef](#)]
24. Zhong, R.; Chen, X.; Lai, C.; Wang, Z.; Lian, Y.; Yu, H.; Wu, X. Drought monitoring utility of satellite-based precipitation products across mainland China. *J. Hydrol.* **2019**, *568*, 343–359. [[CrossRef](#)]
25. Breugem, A.J.; Wesseling, J.G.; Oostindie, K.; Ritsema, C.J. Meteorological aspects of heavy precipitation in relation to floods—An overview. *Earth Sci. Rev.* **2020**, *204*, 103171. [[CrossRef](#)]
26. Brodeur, Z.P.; Steinschneider, S. Spatial Bias in Medium-Range Forecasts of Heavy Precipitation in the Sacramento River Basin: Implications for Water Management. *J. Hydrometeorol.* **2020**, *21*, 1405–1423. [[CrossRef](#)]
27. Islam, M.A. Statistical comparison of satellite-retrieved precipitation products with rain gauge observations over Bangladesh. *Int. J. Remote Sens.* **2018**, *39*, 2906–2936. [[CrossRef](#)]
28. Aslami, F.; Ghorbani, A.; Sobhani, B.; Esmali, A. Comprehensive comparison of daily IMERG and GSMP satellite precipitation products in Ardabil Province, Iran. *Int. J. Remote Sens.* **2019**, *40*, 3139–3153. [[CrossRef](#)]
29. Islam, A.; Yu, B.; Cartwright, N. Assessment and comparison of five satellite precipitation products in Australia. *J. Hydrol.* **2020**, *590*, 125474. [[CrossRef](#)]
30. Lu, D.; Yong, B. A Preliminary Assessment of the Gauge-Adjusted Near-Real-Time GSMP Precipitation Estimate over Mainland China. *Remote Sens.* **2020**, *12*, 141. [[CrossRef](#)]
31. Su, J.; Lu, H.; Ryu, D.; Zhu, Y. The Assessment and Comparison of TMPA and IMERG Products Over the Major Basins of Mainland China. *Earth Space Sci.* **2019**, *6*, 2461–2479. [[CrossRef](#)]
32. Wei, L.; Jiang, S.; Ren, L.; Wang, M.; Zhang, L.; Liu, Y.; Yuan, F.; Yang, X. Evaluation of seventeen satellite-, reanalysis-, and gauge-based precipitation products for drought monitoring across mainland China. *Atmos. Res.* **2021**, *263*, 105813. [[CrossRef](#)]
33. Macharia, J.M.; Ngetich, F.K.; Shisanya, C.A. Comparison of satellite remote sensing derived precipitation estimates and observed data in Kenya. *Agric. For. Meteorol.* **2020**, *284*, 107875. [[CrossRef](#)]

34. Duan, Z.; Liu, J.; Tuo, Y.; Chiogna, G.; Disse, M. Evaluation of eight high spatial resolution gridded precipitation products in Adige Basin (Italy) at multiple temporal and spatial scales. *Sci. Total Environ.* **2016**, *573*, 1536–1553. [[CrossRef](#)]
35. Tian, Y.; Peters-Lidard, C.D.; Adler, R.F.; Kubota, T.; Ushio, T. Evaluation of GSMAp Precipitation Estimates over the Contiguous United States. *J. Hydrometeorol.* **2010**, *11*, 566–574. [[CrossRef](#)]
36. Liu, J.; Shangguan, D.; Liu, S.; Ding, Y.; Wang, S.; Wang, X. Evaluation and comparison of CHIRPS and MSWEP daily-precipitation products in the Qinghai-Tibet Plateau during the period of 1981–2015. *Atmos. Res.* **2019**, *230*, 104634. [[CrossRef](#)]
37. Liu, L.; Wang, Y. Trends in Landfalling Tropical Cyclone-Induced Precipitation over China. *J. Climate* **2020**, *33*, 2223–2235. [[CrossRef](#)]
38. Sun, Q.; Miao, C.; Duan, Q. Changes in the Spatial Heterogeneity and Annual Distribution of Observed Precipitation across China. *J. Climate* **2017**, *30*, 9399–9416. [[CrossRef](#)]
39. Yue, T.-X.; Zhao, N.; Ramsey, R.D.; Wang, C.-L.; Fan, Z.-M.; Chen, C.-F.; Lu, Y.-M.; Li, B.-L. Climate change trend in China, with improved accuracy. *Clim. Change* **2013**, *120*, 137–151. [[CrossRef](#)]
40. Deng, Y.; Gao, T.; Gao, H.; Yao, X.; Xie, L. Regional precipitation variability in East Asia related to climate and environmental factors during 1979–2012. *Sci. Rep.* **2014**, *4*, 5693. [[CrossRef](#)]
41. Su, J.; Lu, H.; Zhu, Y.; Wang, X.; Wei, G. Component Analysis of Errors in Four GPM-Based Precipitation Estimations over Mainland China. *Remote Sens.* **2018**, *10*, 1420. [[CrossRef](#)]
42. Sohoulande, C.D.D.; Stone, K.; Szogi, A.; Bauer, P. An investigation of seasonal precipitation patterns for rainfed agriculture in the Southeastern region of the United States. *Agric. Water Manag.* **2019**, *223*, 105728. [[CrossRef](#)]
43. Sun, Y.; Guan, Q.; Wang, Q.; Yang, L.; Pan, N.; Ma, Y.; Luo, H. Quantitative assessment of the impact of climatic factors on phenological changes in the Qilian Mountains, China. *For. Ecol. Manag.* **2021**, *499*, 119594. [[CrossRef](#)]
44. Che, M.L.; Chen, B.Z.; Innes, J.L.; Wang, G.Y.; Dou, X.M.; Zhou, T.M.; Zhang, H.F.; Yan, J.W.; Xu, G.; Zhao, H.W. Spatial and temporal variations in the end date of the vegetation growing season throughout the Qinghai-Tibetan Plateau from 1982 to 2011. *Agric. For. Meteorol.* **2014**, *189*, 81–90. [[CrossRef](#)]
45. Li, Y.B.; Deng, M.J. Spatiotemporal variations of agricultural water footprint and its economic benefits in Xinjiang, northwestern China. *Sci. Rep.* **2021**, *11*, 23864. [[CrossRef](#)] [[PubMed](#)]
46. Liu, Y.S.; Liu, X.Q.; Liu, Z.J. Effects of climate change on paddy expansion and potential adaption strategies for sustainable agriculture development across Northeast China. *Appl. Geogr.* **2022**, *141*, 102667. [[CrossRef](#)]
47. Zhang, Q.; Han, L.Y.; Zeng, J.; Wang, X.; Lin, J.J. Climate factors during key periods affect the comprehensive crop losses due to drought in Southern China. *Clim. Dyn.* **2020**, *55*, 2313–2325. [[CrossRef](#)]
48. Shi, P.; Sun, S.; Wang, M.; Li, N.; Wang, J.; Jin, Y.; Gu, X.; Yin, W. Climate change regionalization in China (1961–2010). *Sci. China Earth Sci.* **2014**, *57*, 2676–2689. [[CrossRef](#)]
49. Zheng, D. *Ecogeographical Regionalization Research of China*; The Commercial Press: Beijing, China, 2008.
50. Zhou, L.; Sun, H.; Shen, Y. *China's Comprehensive Agricultural Regionalization*; China Agriculture Press: Beijing, China, 1981.
51. Nie, Y.; Sun, J. Evaluation of High-Resolution Precipitation Products over Southwest China. *J. Hydrometeorol.* **2020**, *21*, 2691–2712. [[CrossRef](#)]
52. Kubota, T.; Shige, S.; Hashizurne, H.; Aonashi, K.; Takahashi, N.; Seto, S.; Hirose, M.; Takayabu, Y.N.; Ushio, T.; Nakagawa, K.; et al. Global precipitation map using satellite-borne microwave radiometers by the GSMAp project: Production and validation. *IEEE Trans. Geosci. Remote Sens.* **2007**, *45*, 2259–2275. [[CrossRef](#)]
53. Mega, T.; Ushio, T.; Matsuda, T.; Kubota, T.; Kachi, M.; Oki, R. Gauge-Adjusted Global Satellite Mapping of Precipitation. *IEEE Trans. Geosci. Remote Sens.* **2019**, *57*, 1928–1935. [[CrossRef](#)]
54. Xie, P.; Yatagai, A.; Chen, M.; Hayasaka, T.; Fukushima, Y.; Liu, C.; Yang, S. A Gauge-based analysis of daily precipitation over East Asia. *J. Hydrometeorol.* **2007**, *8*, 607–626. [[CrossRef](#)]
55. Hou, A.Y.; Kakar, R.K.; Neeck, S.; Azarbarzin, A.A.; Kummerow, C.D.; Kojima, M.; Oki, R.; Nakamura, K.; Iguchi, T. The Global Precipitation Measurement Mission. *Bull. Amer. Meteor. Soc.* **2014**, *95*, 701–722. [[CrossRef](#)]
56. Arshad, M.; Ma, X.; Yin, J.; Ullah, W.; Ali, G.; Ullah, S.; Liu, M.; Shahzaman, M.; Ullah, I. Evaluation of GPM-IMERG and TRMM-3B42 precipitation products over Pakistan. *Atmos. Res.* **2021**, *249*, 105341. [[CrossRef](#)]
57. Mou Leong, T.; Santo, H. Comparison of GPM IMERG, TMPA 3B42 and PERSIANN-CDR satellite precipitation products over Malaysia. *Atmos. Res.* **2018**, *202*, 63–76. [[CrossRef](#)]
58. Beck, H.E.; van Dijk, A.I.J.M.; Levizzani, V.; Schellekens, J.; Miralles, D.G.; Martens, B.; de Roo, A. MSWEP: 3-hourly 0.25 degrees global gridded precipitation (1979–2015) by merging gauge, satellite, and reanalysis data. *Hydrol. Earth Syst. Sci.* **2017**, *21*, 589–615. [[CrossRef](#)]
59. Kidd, C.; Levizzani, V. Status of satellite precipitation retrievals. *Hydrol. Earth Syst. Sci.* **2011**, *15*, 1109–1116. [[CrossRef](#)]
60. Hersbach, H.; Bell, B.; Berrisford, P.; Hirahara, S.; Horanyi, A.; Munoz-Sabater, J.; Nicolas, J.; Peubey, C.; Radu, R.; Schepers, D.; et al. The ERA5 global reanalysis. *Q. J. R. Meteorol. Soc.* **2020**, *146*, 1999–2049. [[CrossRef](#)]
61. Chen, Y.; Sharma, S.; Zhou, X.; Yang, K.; Li, X.; Niu, X.; Hu, X.; Khadka, N. Spatial performance of multiple reanalysis precipitation datasets on the southern slope of central Himalaya. *Atmos. Res.* **2021**, *250*, 105365. [[CrossRef](#)]
62. Hong, T.; Li, H.; Chen, M. Comprehensive Evaluations on the Error Characteristics of the State-of-the-Art Gridded Precipitation Products Over Jiangxi Province in 2019. *Earth Space Sci.* **2021**, *8*, e01787. [[CrossRef](#)]
63. Khandu; Awange, J.L.; Forootan, E. An evaluation of high-resolution gridded precipitation products over Bhutan (1998–2012). *Int. J. Climatol.* **2016**, *36*, 1067–1087. [[CrossRef](#)]

64. Xie, P.; Xiong, A.-Y. A conceptual model for constructing high-resolution gauge-satellite merged precipitation analyses. *J. Geophys. Res. D Atmos.* **2011**, *116*, D21106. [\[CrossRef\]](#)
65. Peng, Z.; Li, Y.; Yu, W.; Xing, Y.; Feng, A.; Du, S. Research on the Applicability of Remote Sensing Precipitation Products in Different Climatic Regions of China. *J. Geo-Inf. Sci.* **2021**, *23*, 1296–1311.
66. Kursinski, A.L.; Zeng, X.B. Areal estimation of intensity and frequency of summertime precipitation over a midlatitude region. *Geophys. Res. Lett.* **2006**, *33*, L22401. [\[CrossRef\]](#)
67. Ahmed, K.; Shahid, S.; Wang, X.J.; Nawaz, N.; Khan, N. Evaluation of Gridded Precipitation Datasets over Arid Regions of Pakistan. *Water* **2019**, *11*, 210. [\[CrossRef\]](#)
68. Nkiaka, E.; Nawaz, N.R.; Lovett, J.C. Evaluating global reanalysis precipitation datasets with rain gauge measurements in the Sudano-Sahel region: Case study of the Logone catchment, Lake Chad Basin. *Meteorol. Appl.* **2017**, *24*, 9–18. [\[CrossRef\]](#)
69. AghaKouchak, A.; Behrangi, A.; Sorooshian, S.; Hsu, K.; Amitai, E. Evaluation of satellite-retrieved extreme precipitation rates across the central United States. *J. Geophys. Res. D Atmos.* **2011**, *116*, D02115. [\[CrossRef\]](#)
70. Wang, W.; Lu, H.; Zhao, T.; Jiang, L.; Shi, J. Evaluation and Comparison of Daily Rainfall From Latest GPM and TRMM Products Over the Mekong River Basin. *IEEE J. Sel. Top. Appl. Earth Obs. Remote Sens.* **2017**, *10*, 2540–2549. [\[CrossRef\]](#)
71. Aksu, H.; Akgul, M.A. Performance evaluation of CHIRPS satellite precipitation estimates over Turkey. *Theor. Appl. Climatol.* **2020**, *142*, 71–84. [\[CrossRef\]](#)
72. You, Y.; Wang, N.-Y.; Ferraro, R.; Rudlosky, S. Quantifying the Snowfall Detection Performance of the GPM Microwave Imager Channels over Land. *J. Hydrometeorol.* **2017**, *18*, 729–751. [\[CrossRef\]](#)
73. Shen, Z.; Yong, B.; Gourley, J.J.; Qi, W.; Lu, D.; Liu, J.; Ren, L.; Hong, Y.; Zhang, J. Recent Global Performance of the Climate Hazards Group Infrared Precipitation (CHIRP) with Stations (CHIRPS). *J. Hydrol.* **2020**, *591*, 125284. [\[CrossRef\]](#)
74. Tang, G.; Clark, M.P.; Papalexiou, S.M.; Ma, Z.; Hong, Y. Have satellite precipitation products improved over last two decades? A comprehensive comparison of GPM IMERG with nine satellite and reanalysis datasets. *Remote Sens. Environ.* **2020**, *240*, 111697. [\[CrossRef\]](#)
75. Gao, Z.; Huang, B.; Ma, Z.; Chen, X.; Qiu, J.; Liu, D. Comprehensive Comparisons of State-of-the-Art Gridded Precipitation Estimates for Hydrological Applications over Southern China. *Remote Sens.* **2020**, *12*, 3997. [\[CrossRef\]](#)
76. Ali, H.; Mishra, V. Contributions of Dynamic and Thermodynamic Scaling in Subdaily Precipitation Extremes in India. *Geophys. Res. Lett.* **2018**, *45*, 2352–2361. [\[CrossRef\]](#)
77. Zhang, S.; Wu, J.; Zhao, D.; Xia, L. Characteristics and reasons for light rain reduction in Southwest China in recent decades. *Prog. Phys. Geogr. Earth Environ.* **2019**, *43*, 643–665. [\[CrossRef\]](#)
78. Cinner, J.E.; Caldwell, I.R.; Thiault, L.; Ben, J.; Blanchard, J.L.; Coll, M.; Diedrich, A.; Eddy, T.D.; Everett, J.D.; Folberth, C.; et al. Potential impacts of climate change on agriculture and fisheries production in 72 tropical coastal communities. *Nat. Commun.* **2022**, *13*. [\[CrossRef\]](#)
79. Feng, S.; Hao, Z.; Zhang, X.; Hao, F. Changes in climate-crop yield relationships affect risks of crop yield reduction. *Agricultural and Forest Meteorology* **2021**, *304*, 108401. [\[CrossRef\]](#)
80. Hu, Z.; Wu, Z.; Islam, A.R.M.T.; You, X.; Liu, C.; Li, Q.; Zhang, X. Spatiotemporal characteristics and risk assessment of agricultural drought disasters during the winter wheat-growing season on the Huang-Huai-Hai Plain, China. *Theor. Appl. Climatol.* **2021**, *143*, 1393–1407. [\[CrossRef\]](#)
81. Cong, N.; Wang, T.; Nan, H.; Ma, Y.; Wang, X.; Myneni, R.B.; Piao, S. Changes in satellite-derived spring vegetation green-up date and its linkage to climate in China from 1982 to 2010: A multimethod analysis. *Global Change Biol.* **2013**, *19*, 881–891. [\[CrossRef\]](#)
82. Cao, Q.; Hao, Z.; Yuan, F.; Su, Z.; Berndtsson, R.; Hao, J.; Nyima, T. Impact of ENSO regimes on developing- and decaying-phase precipitation during rainy season in China. *Hydrol. Earth Syst. Sci.* **2017**, *21*, 5415–5426. [\[CrossRef\]](#)
83. Zhang, Q.; Wang, Y.; Singh, V.P.; Gu, X.; Kong, D.; Xiao, M. Impacts of ENSO and ENSO Modoki plus A regimes on seasonal precipitation variations and possible underlying causes in the Huai River basin, China. *J. Hydrol.* **2016**, *533*, 308–319. [\[CrossRef\]](#)
84. Forootan, E.; Khandu; Awange, J.L.; Schumacher, M.; Anyah, R.O.; van Dijk, A.I.J.M.; Kusche, J. Quantifying the impacts of ENSO and IOD on rain gauge and remotely sensed precipitation products over Australia. *Remote Sens. Environ.* **2016**, *172*, 50–66. [\[CrossRef\]](#)
85. Alriah, M.A.A.; Bi, S.; Nkunzimana, A.; Elameen, A.M.; Sarfo, I.; Ayugi, B. Multiple gridded-based precipitation products' performance in Sudan's different topographical features and the influence of the Atlantic Multidecadal Oscillation on rainfall variability in recent decades. *Int. J. Climatol.* **2022**. [\[CrossRef\]](#)
86. Vu, T.M.; Raghavan, S.V.; Liang, S.-Y.; Mishra, A.K. Uncertainties of gridded precipitation observations in characterizing spatio-temporal drought and wetness over Vietnam. *Int. J. Climatol.* **2018**, *38*, 2067–2081. [\[CrossRef\]](#)
87. Power, K.; Axelsson, J.; Wangdi, N.; Zhang, Q. Regional and Local Impacts of the ENSO and IOD Events of 2015 and 2016 on the Indian Summer Monsoon-A Bhutan Case Study. *Atmosphere* **2021**, *12*, 954. [\[CrossRef\]](#)

Disclaimer/Publisher's Note: The statements, opinions and data contained in all publications are solely those of the individual author(s) and contributor(s) and not of MDPI and/or the editor(s). MDPI and/or the editor(s) disclaim responsibility for any injury to people or property resulting from any ideas, methods, instructions or products referred to in the content.